

PREPARATION OF FUNCTIONAL SURFACES USING ZEOLITE
NANOCRYSTALS FOR BIOSENSOR AND BIOMEDICAL APPLICATIONS

A THESIS SUBMITTED TO
THE GRADUATE SCHOOL OF NATURAL AND APPLIED SCIENCES
OF
MIDDLE EAST TECHNICAL UNIVERSITY

BY

SALİH KAAN KİRDECİLER

IN PARTIAL FULFILLMENT OF THE REQUIREMENTS
FOR
THE DEGREE OF MASTER OF SCIENCE
IN
MICRO AND NANOTECHNOLOGY

JULY 2012

Approval of the thesis:

**PREPARATION OF FUNCTIONAL SURFACES USING ZEOLITE
NANOCRYSTALS FOR BIOSENSOR AND BIOMEDICAL
APPLICATIONS**

submitted by **SALİH KAAN KİRDECİLER** in partial fulfillment of the requirements for the degree of **Master of Science in Micro and Nanotechnology Department, Middle East Technical University** by,

Prof. Dr. Canan Özgen
Dean, Graduate School of **Natural and Applied Sciences**

Prof. Dr. Mürvet Volkan
Head of Department, **Micro and Nanotechnology**

Assoc. Prof. Burcu Akata Kurç
Supervisor, **Dept. of Micro and Nanotechnology, METU**

Prof. Dr. Raşit Turan
Co-Supervisor, **Department of Physics, METU**

Examining Committee Members:

Prof. Dr. Hayrettin Yücel
Department of Chemical Eng., METU

Assoc. Prof. Burcu Akata Kurç
Department of Micro and Nanotechnology, METU

Assoc. Prof. Caner Durucan
Department of Metallurgical and Materials Eng., METU

Assist. Prof. Can Özen
Department of Biotechnology, METU

Dr. Kemal Behlülçil
Central Laboratory, METU

Date:

I hereby declare that all information in this document has been obtained and presented in accordance with academic rules and ethical conduct. I also declare that, as required by these rules and conduct, I have fully cited and referenced all material and results that are not original to this work.

Name, Last name: Salih Kaan Kirdeciler
Signature :

ABSTRACT

PREPARATION OF FUNCTIONAL SURFACES USING ZEOLITE NANOCRYSTALS FOR BIOSENSOR AND BIOMEDICAL APPLICATIONS

KİRDECİLER, Salih Kaan

M.Sc., Department of Micro and Nano Technology

Supervisor: Dr. Burcu AKATA KURÇ

Co-Supervisor: Prof. Dr. Raşit TURAN

July 2012, 78 pages

Zeolites are crystalline aluminosilicates which have highly ordered pore structures and high surface area. Also the tailorable surface properties, high ion-exchange capability, high chemical, thermal, and mechanical strength make these particles an important candidate for various application such as sensors, catalysis, dielectric materials, separation, and membrane technologies. Although zeolites have these unique properties, applications where zeolites are integrated into devices according to their application areas, are limited due to the powder form of the material.

The purpose of the current study was to investigate the effect of zeolite nanoparticles on conductometric biosensor performance and cell viability measurements. Firstly, zeolite attachment on silicon surfaces was investigated by attaching silicalite and zeolite A nanoparticles onto the silicon substrates by direct attachment methodology in a closely packed monolayer form with perfect orientation and full coverage without using any chemical linker. Furthermore, the

ability to pattern these zeolite crystals on silicon substrates with electron beam lithography and photolithography techniques was investigated. With the combination of electron beam lithography and direct attachment methodology, zeolite patterns were produced with feature sizes as small as a single silicalite nanoparticle thick line, that is approximately 500 nm. This approach has the ability of patterning very small features on silicon substrate, but the drawback is the long patterning time and lack of electron beam stability during long pattern formation process. Accordingly, it is almost impossible to form large patterns with electron beam lithography systems.

Afterwards, to have full control on surfaces with differentiated areas on solid substrates, patterns of one type of zeolite crystals was formed on the monolayer of another type of zeolite layer with electron beam lithography for the first time. The same closed packed and highly oriented silicalite patterns were successfully formed on zeolite A monolayers and vice versa.

Then photolithography technique was combined with direct attachment methodology to overcome the problem of the lack of total patterned area. With this technique, it was possible to pattern the whole silicon wafer in a couple of seconds, however the feature size of the zeolite patterns was limited with the infrastructures of the mask fabricated for photolithography studies. In this particular study, zeolite lines patterns with a minimum of 5 μm thickness were prepared and the total patterned area was kept constant at 1 cm^2 . Similar to what was obtained by electron beam lithography study, zeolite A patterns were formed on silicalite monolayers with the minimum feature size of 5 μm and vice versa.

In the second part of the study, zeolite films were prepared on the transducers of conductometric biosensors using dip coating technique and named as Zeolite Coated Transducers (ZCT). Electrodes prepared using a mixture of zeolite and enzyme solution and then subjected to casting using glutaraldehyde were called

Zeolite Membrane Transducers (ZMT). The operational and storage stabilities were determined to be in an acceptable range using ZCTs for conductometric urea biosensors. It was observed that using electrodes fabricated by the ZCT technique enhanced the biosensor signals up to two times and showed a rapid response after the addition of urea to the medium when it was compared with Standard Membrane Transducers (SMT). This enhancement can be explained by the lack of GA layer on top of the film, which acts as a diffusion barrier and inhibits the activity of the enzyme. On the second part of this conductometric biosensor study, effect of zeolite modification with methyl viologen (MV) and silver nanoparticles (Ag^+ and Ag^0), as well as the effect of changing Si/Al ratio was investigated with three different zeolite Beta particles which have Si/Al ratios of 40, 50, and 60. There were no significant effect of MV modification on ZMTs and there was no response observed with Ag^+ and Ag^0 modified zeolites. However, it was observed that conductometric responses increased with increasing Si/Al ratio for ZMTs. This behavior can be due to an increased hydrophobicity and/or the increasing acidic strength with the increasing Si/Al ratio within the zeolite crystals. Also ZCTs showed higher responses with respect to both SMTs and ZMTs. When compared with SMTs and ZMTs, ZCTs had higher reproducibility due to the controlled thickness of zeolite thin film by dip coating, and the controlled amount of enzyme adsorbed on this film.

In the third part of the study, effect of zeolites on cell proliferation with MG63 osteoblast cells and NIH3T3 fibroblast cells were investigated. For that purpose, zeolite A, silicalite, and calcined forms of these zeolites were patterned with photolithography technique onto silicon wafers. Three different patterns prepared for this particular study, which has 0.125cm^2 , 0.08825cm^2 , and 0.04167cm^2 zeolite patterned areas on 1cm^2 samples. In that way, not only the zeolite type and effect of calcination of zeolites, but also the effect of zeolite amount on MG63 osteoblast cells and NIH3T3 fibroblast cells were investigated.

Silicalite coated samples were observed to have higher amount of cells than zeolite A coated samples after 24, 48, and 72 hours of incubation. This may be referred to the hydrophilic/hydrophobic properties, surface charge, and/or particle size of zeolites. Also it is observed that higher zeolite amount on samples resulted in an increase in the number of cells attached to the samples.

There was also a significant increase in the number of cells upon using calcined silicalite samples. Accordingly, it can be hypothesized that zeolite pores result in an enhancement of protein adsorption and proliferation, even if this only occurs at the pore openings. On the other hand, there was no positive effect of calcining zeolite A. This result was expected since there is no structure directing agent used in synthesis procedure of zeolite A, which again supports the fact that pores might have some role in cell attachment.

Keywords: Zeolite, Patterning, Electron Beam Lithography, Photolithography, Cell Viability, Conductometric Biosensor

ÖZ

BİYOSENSÖR VE BİYOMEDİKAL UYGULAMALAR İÇİN ZEOLİT NANOKRİSTALLERİ KULLANILARAK FONKSİYONEL YÜZEYLERİN OLUŞTURULMASI

KİRDECİLER, Salih Kaan

Yüksek Linsans, Mikro ve Nanoteknoloji Bölümü

Tez Yöneticisi : Doç. Dr. Burcu AKATA KURÇ

Ortak Tez Yöneticisi: Prof. Dr. Raşit TURAN

Temmuz 2012, 78 sayfa

Zeolitler düzenli gözenek yapıları sebebiyle çok yüksek yüzey alanına sahip kristalin alüminasilikatlardır. Ayrıca değiştirilebilir yüzey özellikleri, yüksek iyon değiştirebilme özelliği, kimyasal, ısı ve mekanik dayanım özellikleri bu malzemeleri sensör cihazları, kataliz, dielektrik malzemeler, ayrıştırma ve membran teknolojilerinde kullanılmak üzere önemli bir aday kılmaktadır. Bu kadar eşsiz özelliğine rağmen, zeolitlerin uygulama alanlarına göre cihazlara entegrasyonu toz formu yüzünden sınırlı kalmıştır.

Bu çalışmanın amacı zeolite nanoparçacıklarının kondüktometrik biyosensör performansına ve hücre çoğaltma çalışmalarındaki etkisini gözlemlemektir. İlk olarak, zeolitlerin silikon yüzeylere doğrudan tutturma yöntemi ile film yapımı araştırılmış olup, silikalit ve zeolit A parçacıkları sıkı bir şekilde tek katmanlı, tam düzenli ve tam kaplı zeolit filmleri herhangi bir kimyasal kullanılmadan oluşturuldu. Ardından, bu zeolitlerin silikon yüzeyler üzerinde elektron demet

litografisi ve fotolitografi yöntemleri ile desen oluşturma kabiliyeti incelenmiştir. Elektron demet litografisi ve doğrudan tutturma yönteminin kombinasyonu ile, tek bir silikalit çapı kadar çok küçük desen kalınlığında çizgiler üretilmiştir. Bu yöntem ile çok küçük ebatlardaki desenler oluşturulabilmekle beraber uzun süren desen oluşturma işlemi ve bu işlem süresinde elektron demetinin stabilitesinin kaybolması gibi dezavantajları bulunmaktadır. Bu sebeplerden dolayı, elektron demet litografisi ve direk tutturma yöntemi ile geniş ve büyük desenler oluşturmak neredeyse imkansızdır.

Ardından, yüzeyler üzerinde tam anlamıyla kontrole sahip olarak değiştirilmiş alanlar oluşturabilmek için zeolit tek katman tabakası üzerine bir başka zeolitten desenler ilk kez oluşturulmuştur. Aynı düzenli, sıkı ve tam kaplı silikalit desenleri, tek katman zeolit A filmi üzerine, zeolit A desenleri ise, tek katman silikalit filmleri üzerinde oluşturulmuştur.

Elektron demet litografisi yönteminin ardından fotolitografi yöntemi ile doğrudan tutturma yöntemi ile birleştirilerek toplam desen alanı konusundaki sorun çözülmüştür. Bu yöntem ile tüm silikon gofret üzerine birkaç saniye içerisinde desen oluşturulabilmektedir, ancak bu durumda ise fotolitografi sisteminde kullanılan maskenin, üretim sırasında ulaşılabilen altyapı kaynakları sebebiyle desen boyutları limitleyici faktör olmaktadır. Bu çalışma için toplam alanı 1 cm^2 olan örnekler hazırlanıp, en düşük $5 \text{ }\mu\text{m}$ kalınlıkta zeolit desenleri oluşturulmuştur. Elektron demet litografisi ile yapıldığı gibi, fotolitografi yöntemi ile tek katman zeolit A filmi üzerine silikalit desenleri üretilmiş, tek katman silikalit filmi üzerine zeolit A desenleri minimum desen boyutu $5 \text{ }\mu\text{m}$ olacak şekilde üretilmiştir.

Çalışmanın ikinci kısmında, kondüktometrik biyosensör yüzeyleri üzerine daldırarak kaplama metodu ile zeolit filmleri oluşturulmuş ve bu tip transdüserler zeolit kaplı transdüser olarak adlandırılmıştır. Zeolitin enzim solüsyonu ile

karıştırılması ardından glutaraldehid ile membran oluşturularak hazırlanan transdüserler ise zeolit membran transdüser olarak adlandırılmıştır. Zeolit kaplı transdüser ve zeolit membran transdüserlerin operasyonel ve bekleme stabilite değerleri kondüktometrik biyosensörler için kabul edilebilir seviyede olduğu görülmüştür. Zeolit kaplanarak üretilen transdüserlerin standard membran transdüserlerle karşılaştırıldığında sinyalleri iki kata kadar artırdığı ve üretilmesinin hemen ardından çok hızlı bir sinyal değişimi gösterdiği gözlemlenmiştir. Bu artış, filmlerin üzerinde difüzyon bariyeri olarak düşünülebilecek ve enzimeleri inhibe edebilen glutaraldehid tabakası bulunmaması ile açıklanabilir. Kondüktometrik biyosensör çalışmasının ikinci aşamasında Si/Al oranı 40, 50 ve 60 olan zeolit Beta örnekleri ile metilviolen (MV), gümüş iyonu ve gümüş nanoparçacık (Ag^+ ve Ag^0) modifikasyonlarının etkisi araştırılmıştır. MV modifikasyonunun kondüktometrik tepki üzerine kaydedeğer bir etkisi görülmemekle beraber, Ag^+ ve Ag^0 modifikasyonlu örneklerden herhangi bir sinyal alınamamıştır. Ancak kondüktometrik sinyallerin zeolit membran transdüserlerde artan Si/Al ile arttığı gözlemlenmiştir. Bu değişim zeolit içerisinde artan Si/Al oranları sonucunda artan hidrofobik özellikler ve/veya artan asidik özellikler ile açıklanabilir. Ayrıca zeolit kaplı transdüserler, standard membran transdüserler ve zeolit membran transdüserlerden daha yüksek sinyal vermiştir. Zeolit kaplı transdüserler, daldırarak kaplama sistemi ile kaplandığı ve bu kaplama yönteminde kaplama kalınlığı kontrol edilebildiğinden ve istenilen oranda enzimin absorblanabilmesi sebebiyle zeolit membran transdüserler ve standard membran transdüserler ile karşılaştırıldığında tekrarlanabilirliği daha fazladır.

Çalışmanın üçüncü aşamasında, zeolitlerin MG 63 osteoblast hücrelerinin ve NIH 3T3 fibroblast hücrelerinin büyümeleri üzerine etkisi araştırılmıştır. Bu amaçla, zeolite A, silikalit ve bu zeolitlerin kalsine formları ile fotolitografi tekniği kullanılarak silikon gofretler üzerine desenler oluşturulmuştur. Bu çalışma için üç

değişik desen hazırlanmış olup toplam alanı 1 cm^2 olan örnekler üzerinde 0.125 cm^2 , 0.08825 cm^2 ve 0.04167 cm^2 zeolit kaplı alanlar oluşturulmuştur. Bu sayede sadece zeolit türünün ve kalsinasyon etkisi değil, aynı zamanda zeolit miktarının MG 63 osteoblast hücrelerinin ve NIH 3T3 fibroblast hücrelerinin çoğalması üzerine etkisi de incelenmiştir.

Silikalit kaplı örnekler üzerinde, zeolit A kaplı örneklerden 24, 48 ve 72 saatlik inkübasyonun ardından daha fazla hücre bulunduğu gözlemlenmiştir. Bu zeolitin hidrofilitik/hidrofobik özelliklerindeki, yüzey yükündeki ve/veya parçacık boyutunun farkından kaynaklanabilir. Ayrıca örnekler üzerindeki zeolit miktarındaki artışın, yüzeydeki toplam hücre sayısında artışa sebebiyet verdiği belirlenmiştir.

Silikalit örnekleri dikkate alınarak kalsinasyonun etkisine bakıldığında hücre sayısında ciddi bir artış görülmüştür. Bu durumda, zeolit gözeneklerinin, en azından yüzeydeki gözenek açıklıklarının, besiyerinde bulunan proteinlerin adsorpsiyonunu artırdığı, dolayısıyla daha yüksek hücre tutunumu ve çoğalması gerçekleştiği şekilde açıklanabilir. Diğer taraftan, zeolit A ile kalsinasyon etkisi gözlemlenmemiş olup, bunun sebebi zeolit içerisinde yapı yönlendirici ajanların sentez prosedürü içerisinde kullanılmamış olması şeklinde açıklanırken, gözeneklerin hücre çoğalması üzerine etkisini desteklemiştir.

Anahtar Kelimeler: Zeolit, Desen Oluşturma, Elektron Demet Litografisi, Fotolitografi, Hücre Çoğalımı, Kondüktometrik Biyosensör

to my lovely family...

ACKNOWLEDGEMENTS

First and foremost I offer my sincerest gratitude to my supervisor, Dr. Burcu Akata, who has supported me throughout my thesis with her patience and knowledge whilst allowing me the room to work in my own way. Her supervision, advice, and guidance from the very early stage of this research as well as giving me extraordinary experiences through out the work. Above all and the most needed, she provided me unflinching encouragement and support in various ways. Also I would like to thank to my co-supervisor Prof. Dr. Raşit TURAN for supporting this work with his laboratory facilities and scientific ideas.

Furthermore, I would like to thank to the rest of my thesis committee; Prof. Dr. Hayrettin Yücel, Dr. Caner Durucan, Dr. Can Özen and Dr. Kemal Behlülgil for their valuable comments.

I would also like to thank to METU Central Laboratory, for enabling its wide facilities anytime needed in this work, also I would like to thank the members of my research group, Sezin Galiođlu Özalтуđ, Esin Soy Yapıcı, Seçkin Öztürk, Sedat Canlı, Berna Ozansoy Kasap, Mehmet Koç and Melda İşler for their precious guidance, inspiration, supports, and helps during my research stays abroad. I also thank İ. Özgür Erişen, İlker Yıldız, Hikmet Eren, Leyla Karabey Molu, Eda Ayşe Aksoy, Serap Tekin, Uđur Özgürgül and Levent Yıldız for their supports in Central Laboratory and Biotechnology Research Center. I owe my gratitude to Dr. Juliusz Warzywoda, Prof. Dr. Albert Sacco Jr., Prof. Dr. Sergei V. Dzyadevych, Prof. Dr. Alexey Soldatkin, Dr. Oleksandr Soldatkin, Dr. Cathy Tkaczyk and Prof. Dr. Maryam Tabrizian for their helps and advice during my study.

I also wish to express my love and gratitude to all *my family members*, Ali Kirdeciler, Zehra Kirdeciler, İhsan Utkan Kirdeciler, and my firends whom i can say my brothers Emre Erdal, Özgür Küçük, Berk Baltacı, Görkem Gümüşsoy, Orhan Vardar, Serdar Aşkar and Gözde Yayla Aşkar for their faithful support, love and encouragement during my whole study.

Last, but not least, my deepest gratitude goes to Eda Naifoğlu for her sacrifice, personal support and great patience at all times. She always gives me warm encouragement and love in every situation. Her support and encouragement was in the end what made this dissertation possible.

I am also appreciative of the financial support that I received for this study through Scientific and Technical Research Council of Turkey (TUBITAK) and European Union project with the project number PIRSES-GA-2008-230802.

TABLE OF CONTENTS

ABSTRACT.....	iv
ÖZ.....	viii
ACKNOWLEDGEMENTS.....	xiii
TABLE OF CONTENTS.....	xv
LIST OF FIGURES.....	xix
LIST OF TABLES.....	xxiii
LIST OF SYMBOLS.....	xxiv
CHAPTERS	
1.INTRODUCTION.....	1
1.1 Zeolite and Zeo-type Materials.....	1
1.1.1 Structure of Zeolites.....	1
1.1.2 Protein Immobilization on Zeolites.....	3
1.1.3 Cell Viability Studies with Zeolites.....	4
1.2 Biosensors.....	6
1.2.1 Conductometric Biosensors.....	7
1.2.1.1 Measurement Setup.....	9
1.2.1.2 Conductometric Urea Biosensors.....	10

1.2.2 Zeolites for Biosensor Applications.....	11
1.3 Cell Viability.....	13
2. LITERATURE REVIEW.....	15
2.1 Zeolite Thin Films.....	16
2.2 Forming Controlled Zeolite Patterns on Solid Substrates.....	19
2.3 Enzyme Immobilization and Biosensor Studies on Zeolites.....	21
2.4. Cell Viability with Zeolites.....	23
3.EXPERIMENTAL.....	25
3.1 Synthesis of Zeolite and Zeo-type Materials	25
3.1.1 Synthesis of Zeolite A.....	25
3.1.2 Synthesis of Zeolite Beta with Varying Si/Al Ratio.....	26
3.1.3 Synthesis of Silicalite.....	26
3.2 Modification of Zeolites.....	27
3.2.1 Ion Exchange of Zeolite Beta with Ag	27
3.2.2 Reduction of Ag-ion exchanged Zeolite Beta	27
3.2.3 Modification with methyl viologen.....	28
3.3 Attachment and Patterning of Zeolites on Solid Substrate.....	28
3.3.1 Attachment of Zeolites on Conductometric Biosensor Electrodes.....	28
3.3.2 Attachment of Zeolites on Silicon Surfaces.....	30

3.3.3 Zeolite Patterning with Electron Beam Lithography.....	31
3.3.4 Zeolite Patterning with Photolithography.....	32
3.4 Cell Viability Measurements.....	34
3.4.1 MTT assays with MG63 Cell Lines.....	34
3.4.2 MTT assays with NIH3T3 Cell Lines.....	35
3.5 Material Characterization	35
3.5.1 X-Ray Diffraction (XRD).....	35
3.5.2 Scanning Electron Microscopy (SEM).....	36
3.5.3 Particle Size Analysis.....	36
3.5.4 Contact Angle Measurements.....	36
3.5.5. Pore Size Distribution.....	37
3.6 Conductometric Biosensor Measurements.....	37
4. RESULTS AND DISCUSSION.....	38
4.1 Synthesis, Characterization and Modification of Zeolite and Zeo-type Materials	38
4.1.1 Zeolite A.....	38
4.1.2 Zeolite Beta with Varying Si/Al Ratio.....	40
4.1.3 Silicalite	43
4.2 Modification of Zeolites with Silver and Methylviologen.....	45

4.3 Zeolite Attachment and Patterning.....	46
4.3.1 Attachment of Zeolites on Conductometric Biosensor Electrodes.....	46
4.3.2 Attachment of Zeolites on Silicon Substrates	47
4.3.3 Zeolite Patterning with Electron Beam Lithography.....	49
4.3.4 Zeolite Patterning with Photolithography.....	51
4.4 Cell Viability Measurements.....	53
4.4.1 MTT assays with MG63 Cell Lines.....	54
4.4.2 MTT assays with NIH3T3 Cell Lines.....	58
4.5 Conductometric Biosensor Measurements.....	63
4.5.1 Response Characteristics of Silicalite Modified Electrodes.....	63
4.5.2 Operational and Storage Stabilities of Silicalite Modified Electrodes.....	66
4.5.3 Effect of Si/Al ratio on Conductometric Urea Biosensors.....	69
4.5.4 Effect of Zeolite Modification with Silver and MV on Conductometric Urea Biosensors.....	73
5. CONCLUSION.....	75
REFERENCES	79
APPENDICES	
A. Literature XRD diffractograms	86
B. Representative scanning electron microscopy images of prepared various zeolite patterns.....	89

LIST OF FIGURES

FIGURES

Figure 1.1 Primary building units of zeolites	2
Figure 1.2 Framework structures of zeolite A (A), silicalite (B), and zeolite Beta(C)	2
Figure 1.3 Schematic of a simple biosensor.....	6
Figure 1.4 Schematic representation of conductometric biosensor system.....	9
Figure 1.5 The conductometric biosensor system at METU.....	9
Figure 1.6 Schematic representation of mitochondrial reaction of MTT.....	14
Figure 3.1 Schematic representation of electrodes; (A) Standard Membrane Transducer (SMT), (B) Zeolite – Membrane Transducer (ZMT), (C) Zeolite Coated Transducer (ZCT).....	30
Figure 3.2 Schematic representation of zeolite patterning procedure with EBL..	31
Figure 3.3 Schematic representation of zeolite patterning procedure on top of a zeolite monolayer with EBL.....	32
Figure 3.4 Schematic representation of zeolite patterning procedure with PL.....	33
Figure 3.5.Schematic representation of zeolite patterning procedure on top of a zeolite monolayer with PL.....	34
Figure 4.1 XRD diffractograms of the synthesized zeolite A particles.....	39
Figure 4.2 Scanning electron microscopy images of zeolite A particles.....	40

Figure 4.3 XRD diffractograms of the synthesized zeolite Beta particles.....	41
Figure 4.4 Scanning electron microscopy images of zeolite Beta particles with Si/Al ratio of 40 (A), 50 (B) and 60 (C).....	42
Figure 4.5 XRD diffractograms of the synthesized silicalite particles.....	43
Figure 4.6 Scanning electron microscopy images of silicalite particles.....	44
Figure 4.7 Scanning Electron Microscopy images of the Zeolite Coated Transducers (ZCT) with Silicalite (A) and Zeolite Beta Si/Al ratio of 60 (B).....	47
Figure 4.8 Scanning electron microscopy images of s of zeolite A (A) and silicalite (B) monolayers formed by direct attachment on silicon substrate.....	48
Figure 4.9 Scanning electron microscopy images of zeolite A monolayer patterns formed by EBL.....	49
Figure 4.10 Scanning electron microscopy images of zeolite A line patterns on silicalite monolayer (A) and silicalite line patterns on zeolite A monolayers (B) formed by EBL.....	50
Figure 4.11 Scanning electron microscopy images of two different zeolite A pattern formations prepared with PL.....	51
Figure 4.12 Scanning electron microscopy images of zeolite A cross-line patterns on silicalite monolayer (A) and silicalite cross-line patterns on zeolite A monolayer (B) formed by PL.....	52
Figure 4.13 MTT assay results for various samples after 24, 48, and 72 hours of incubation for MG63 Cell Line with 0.125 cm ² zeolite coated samples.....	54
Figure 4.14 MTT assay results for various samples after 24, 48, and 72 hours of incubation for MG63 Cell Line with 0.08825 cm ² zeolite coated samples.....	55

Figure 4.15 MTT assay results for various samples after 24, 48, and 72 hours of incubation for MG63 Cell Line with 0.04167 cm² zeolite coated samples.....55

Figure 4.16 MTT assay results for various samples with 0.125, 0.08825, and 0.04167 cm² zeolite patterned area for MG63 Cell Line for 24 hours incubation.....56

Figure 4.17 MTT assay results for various samples with 0.125, 0.08825, and 0.04167 cm² zeolite patterned area for MG63 Cell Line for 48 hours incubation.....57

Figure 4.18 MTT assay results for various samples with 0.125, 0.08825, and 0.04167 cm² zeolite patterned area for MG63 Cell Line for 72 hours incubation.....57

Figure 4.19 MTT assay results for various samples for 24, 48, and 72 hours of incubation for NIH 3T3 Cell Line with 0.125 cm² zeolite coated samples.....59

Figure 4.20 MTT assay results for various samples for 24, 48, and 72 hours of incubation for NIH 3T3 Cell Line with 0.08825 cm² zeolite coated samples.....59

Figure 4.21 MTT assay results for various samples for 24, 48, and 72 hours of incubation for NIH 3T3 Cell Line with 0.04167 cm² zeolite coated samples.....60

Figure 4.22 MTT assay results for various samples with 0.125, 0.08825, and 0.04167 cm² zeolite patterned area for NIH 3T3 Cell Line for 24 hours incubation.....61

Figure 4.23 MTT assay results for various samples with 0.125, 0.08825, and 0.04167 cm² zeolite patterned area for NIH 3T3 Cell Line for 24 hours incubation.....61

Figure 4.24 MTT assay results for various samples with 0.125, 0.08825, and 0.04167 cm ² zeolite patterned area for NIH 3T3 Cell Line for 24 hours incubation.	62
Figure 4.25 Comparison of response curves obtained for ZCT with SMT for urea determination for conductometric biosensors.....	64
Figure 4.26 Response curves of conductometric biosensor based on urease ZCT and SMT.....	65
Figure 4.27 Operational (A) and storage (B) stability results of ZCTs with Silicalite.....	67
Figure 4.28 Comparison of responses obtained using ZMT's prepared using BEA40, BEA50 and BEA60 and SMT type conductometric biosensors.....	70
Figure 4.29 Comparison of the calibration curves between SMT, ZMT, and ZCTs using zeolite BEA50 (A) and BEA60 (B).....	72
Figure A.1 Literature XRD diffractograms of zeolite A.....	86
Figure A.2 Literature XRD diffractograms of zeolite Beta.....	87
Figure A.3 Literature XRD diffractograms of Silicalite.....	88
Figure B.1 Representative scanning electron microscopy images of prepared various zeolite patterns.....	89
Figure B.2 Representative scanning electron microscopy images of prepared various zeolite patterns.....	90

LIST OF TABLES

TABLES

Table 4.1 Surface properties of zeolite Beta crystals.....	41
Table 4.2 Properties of ion exchanged sub-micron zeolite Beta crystals.....	46
Table 4.3 The Contact Angle Measurements of zeolite monolayers.....	49
Table 4.4 Effect of zeolite modification on Conductometric Biosensor Transducers.....	74

LIST OF SYMBOLS

BEA: Zeolite Beta

GA: Glutaraldehyde

PDMS: Polydimethylsilane

SMT: Standard Membrane Transducers

ZMT: Zeolite Membrane Transducers

ZCT: Zeolite Coated Transducers

BSA: Bovine Serum Albumin

PBS: Phosphate Buffer Solution

EBL: Electron Beam Lithography

PL: Photolithography

XRD: X-Ray Diffraction

MV: Methylviologen

CHAPTER 1

INTRODUCTION

1.1 Zeolite and Zeo-type Materials

1.1.1 Structure of Zeolites

Zeolites are crystalline aluminosilicates with three dimensional frameworks which form highly ordered uniform pore structures. Zeolite framework consists of primary building units (TO_4), where T atoms are tetrahedrally coordinated silicon or aluminum atoms that are connected to each other through oxygen atoms. Crystallographic unit cell of a zeolite can be represented by $M_{x/n}[(AlO_2)_x(SiO_2)_y] \cdot wH_2O$ where n represents the valence of cation M, x and y represents the total number of tetrahedra per unit cell and w represents the number of water molecules in a single unit cell. The complex structure of zeolites are based on infinitely extending three dimensional, four connected framework of linked AlO_4 and SiO_4 tetrahedra with sharing oxygen ions. AlO_4 tetrahedron in the framework bears a net negative charge which is balanced by an extra framework cation which is usually sodium. Schematic representation of these primary building units and the framework types are shown in Figure 1.1 and Figure 1.2 respectively. These structures contain uniform pore with the size range

of 4-13 Å. Zeolites synthesized by hydrothermal synthesis where transport mechanism involves the diffusion of aluminate, silicate, and/or aluminosilicate species from the liquid phase to the nucleation site for crystal growth. In the synthesis of some zeolites, structure directing agents are used to build the primary building units and form the crystalline structure. These structure directing agents are organic guest molecules and they can be cleaned by calcination process [1].

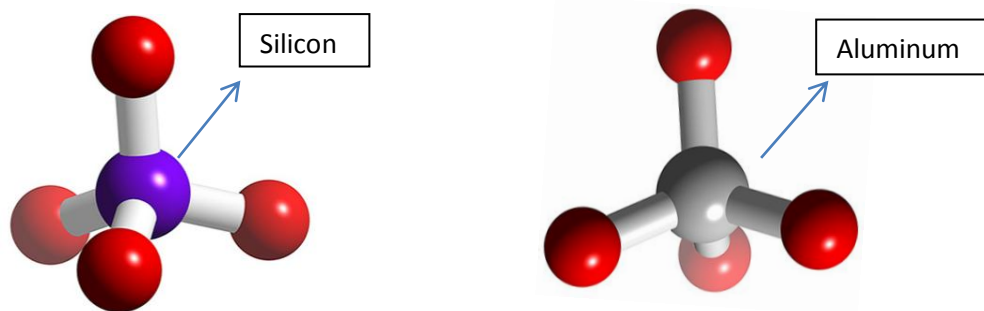


Figure 1.1 Primary building units of zeolites [2].

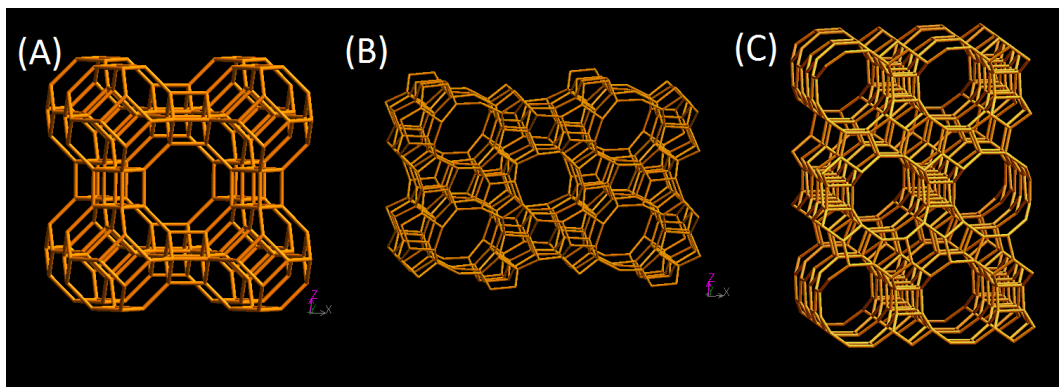


Figure 1.2 Framework structures of zeolite A (A), silicalite (B), zeolite Beta (C).

*Taken from iza-structure.org.

It is possible to synthesize zeolites in desired particle sizes by changing the synthesis parameter such as concentration of Si and Al sources, reaction time, and aging time. In that way, it is possible to investigate the effect of zeolite parameters such as Si/Al ratio, particle size, total surface area, and internal surface area without changing the pore size and zeolite structure [3]. Obtaining zeolites with varying Si/Al ratios lead to different acidic and hydrophilic/hydrophobic properties without changing any other zeolitic property, which would allow one to investigate the effect of such parameters in applications for which these parameters can be very important, such as biosensors and protein adsorption [2, 4].

As-synthesized zeolites have –OH groups connected to Al and Si atoms which are called Brønsted acid sites (Al-OH-Si) and Si atoms which are called silanol groups (Si-OH) [1]. These OH groups can be exchanged with various groups such as -NH_4^+ and -H^+ depending on the application area. Examples of this type can be given from the studies of Soy et al., where NH_4^+ -Beta 25 zeolite modified conductometric biosensors had similar responses compared to traditional enzyme membrane approach with conductometric glucose oxidase immobilized biosensors [5] while in a study performed by Sárkány et al., water uptake capability varied with the surface groups of the zeolites [6].

1.1.2 Protein Immobilization on Zeolites

Protein immobilization studies on different substrates are highly important for various applications such as biosensors, protein separations, and carrier applications. Immobilization processes can be classified in three groups, which are cross-linking with a material such as glutaraldehyde (GA), entrapment of proteins in a matrix, and adsorption of proteins on supports.

Among these processes, there can be several disadvantages of cross-linking and entrapment approaches. One disadvantage is that the chemical used to cross-link or entrap the enzyme can damage the enzyme and result in a decrease in enzyme activity and stability.

Another approach, which is adsorption of proteins on supports, has the disadvantage of protein leakage in a medium caused by the weak interaction of protein and support such as van der Waals forces, hydrogen bonding or electrostatic forces. Nevertheless, this approach is relatively simpler and cheaper, and there is usually no need for further treatment on the support [7].

Zeolite crystals are among the most promising candidates as a support for enzyme adsorption, since they have very large surface area, controllable surface groups, particle size, shape and three dimensional ordered pore structures. The most important approach for using zeolites as supports would be the need to attach these, nanometer to micrometer particle size crystals on a decent substrate in order to gain full control over further adsorption studies and most importantly to turn these components into miniaturized devices. There can be several interactions that can be significant once proteins come in close contact with a zeolite nanoparticle. These can be columbic attractions, hydrophilic/hydrophobic interactions and van der Waals interactions. These interactions are highly dependent on the medium properties and surface groups of the zeolite.

1.1.3 Cell Viability Studies with Zeolites

There is an increasing interest in the modification of the micro-environment of the cells that results in enhanced proliferation and viability, which can be very

important for implant technologies and bio-applications. In that sense, it can be very interesting to investigate the potential use of zeolites to study whether there would be any change in the obtained cell adhesion, proliferation and differentiation due to zeolites' biocompatibility and large surface area as well as their tunable surface groups.

Osteoblast proliferation and differentiation is very important for bone regeneration studies in implants [8]. Zeolites are one of the potential candidates for alternative materials as implants, due to their 3D microstructures formed with an excellent network of sub-nanometer sized pores along with their unique topography that makes zeolites suitable for bone cell adhesion, proliferation and growth [8-10]. An example can be given for zeolite A, which was found to have potential for influencing bone formation by its effect on osteoblasts [11].

Fibroblasts are another class of cells that are very important for body, since these cells are responsible for the synthesis of extracellular matrix and collagen. There are several studies about the enhancement of fibroblast proliferation [12]. Zeolites are again an important candidate since they are non-toxic for fibroblasts and they did not affect the morphology of the cells [13].

Accordingly, in the current thesis study, an array of line varying in size composed of zeolites were patterned on silicon substrates to investigate the effect of zeolite patterns on cellular behavior of osteoblasts and fibroblasts. In this way, it was possible to gain full control over the zeolite amount and type that are of crucial importance for cell proliferation and viability. Furthermore, the effect of calcining zeolites that leads to cleaner and open pore structure with increased internal surface area was also investigated.

1.2 Biosensors

The interest of the development in analytical devices for detection, quantification and monitoring of specific chemical species has led to an emerge of biosensors. The estimation of various metabolites like urea, glucose, and cholesterol in blood is one of the most important researches in clinical diagnostic area. Biosensors represented a new trend on this research area [14]. Biosensors are basically a sub-unit of chemical sensors, which recognition system utilizes a biochemical mechanism [15]. This system translates information that come from biochemical domain which is usually analyte concentration into a physical output signal with a defined sensitivity. While all biosensors are more or less selective to a particular analyte, the main purpose of the recognition systems is to provide higher selectivity [15]. Biosensors are usually specific, rapid, simple to use and fabricate, and the most importantly minimal sample usage devices. The combination of two totally different disciplines such as sensitivity and specificity of biological systems and high computing properties of computer technology leads these biosensor systems [14]. General schematic of the biosensor systems shown in Figure 1.3.

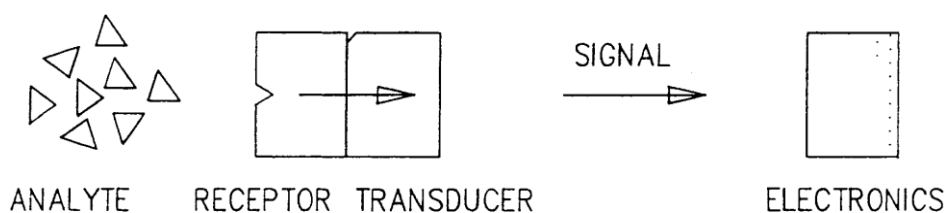


Figure 1.3 Schematic of a simple biosensor [14].

Biosensors are inexpensive tools for biomolecule detection with high selectivity and fast response properties. These sensors are becoming an indispensable element with these amazing properties, even though, these biosensors are still being developed for further applications.

Biomolecules in the body fluids can be determined by these systems for the detection of diseases, infections, intoxications, etc. Also with the help of biosensors, level of these biomolecules in body fluids, the level of the infection or diseases can be determined. Also the agricultural products are needed to be investigated with these systems for the food quality and healthiness. Moreover, some mid-products or by-products of industrial processes needed to be monitored for the quality management of these production lines. Even there are several significantly sensitive characterization devices such mass spectrometer and chromatography systems but these systems are slow, expensive and big . For all these reasons, there is a huge interest on biomolecule detection with biosensors in an easy, fast and inexpensive way.

1.2.1 Conductometric Biosensors

Conductometric biosensors measure the conductivity of the solution. Almost every solution has positively charged cations and negatively charged anions. When two metal wires dipped into a solution and an electric field is induced by an applied potential, cations move along negative side, while anions move along the positive site. The movement of these ions in the solution leads to a measurable current and with the help of Ohm's law, conductivity of the solution can be measured.

$$S = I/V \quad (1.1)$$

In the equation S is the conductivity while V is the applied potential and I is the induced current. Conductivity of the solution at a specific time can be calculated from the following equation.

$$X = (SL)/A \quad (1.2)$$

In this equation X is the specific conductivity where L is the distance between the metal wires and A is the total metal solution interface. There are several more parameters affecting the conductance, and these parameters can be represented as a constant C, X can be given as:

$$X = C \sum(u_i c_i) \quad (1.3)$$

In this equation, u_i is the mobility and c_i is the concentration of ions while C is the parameters explained above. While the enzymatic reaction takes place, the values of u_i and c_i changes. The result of this reaction is consumption or production of ions which can be measured as a variant of X as an indicator of the reaction.

1.2.1.1 Measurement Setup

Measurement setup consists of a function generator, lock in amplifier, a computer, and a conductometric biosensor transducer. The schematic representation of the setup and photograph of the setup is given in Figure 1.4 and 1.5 respectively.

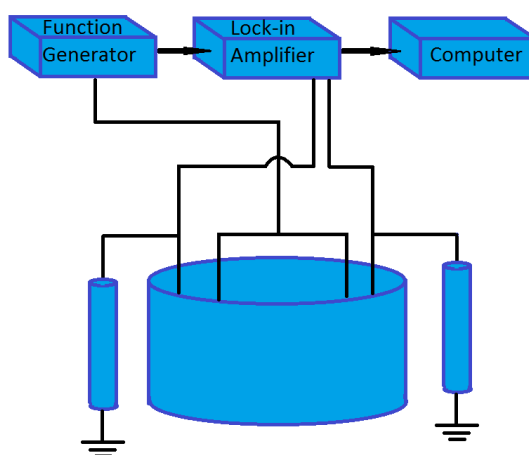


Figure 1.4 Schematic representation of conductometric biosensor system.

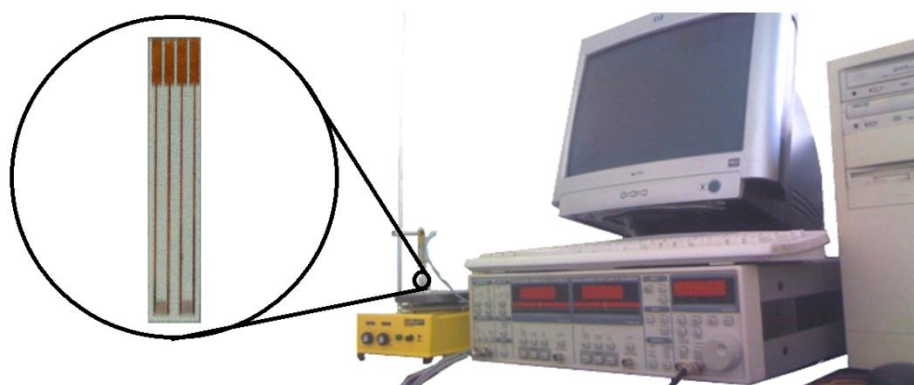


Figure 1.5 The conductometric biosensor system at METU.

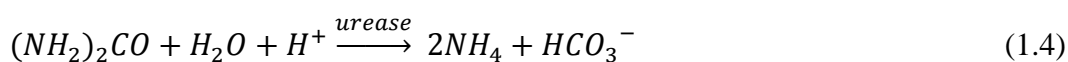
The most important advantage of the conductometric biosensors are the low cost of fabrication due to the simple structure of the transducers. This type of biosensor indirectly measures the enzymatic reaction, by measuring the conductivity of the solution. The most important disadvantage of this system is the low selectivity, due to the background conductivity of the solution.

1.2.1.2 Conductometric Urea Biosensors

Urea determination in biological liquids is an important diagnostic test as the increase in urea concentration in blood and its decrease in urine actually evidence to renal dysfunction of the organism. Basically, standard methods of determination of urea concentration in biological liquids use direct color reactions with spectrophotometric indexation of ammonium, generated as a result of catalytic urea disintegration by urease. These methods include complex and fine procedures and consume long time. Besides, use of spectrophotometry is rather restricted for color solutions like blood.

However, urease biosensors are not widely used in practice. The matter is that they are not sufficiently sensitive and stable, and moreover, the linear range of measurable concentrations is rather narrow. There are several studies to overcome these drawbacks of conductometric urease sensors, and modification of biosensor electrodes with zeolites, is one of the candidate for this situation.

The conductometric responses of such electrodes modified with zeolites were tested using the enzymatic reaction of urease:



This reaction results in a change of charged ions which results in local alteration of conductivity in the solution. This allows usage of conductometric electrodes as transducers.

1.2.2 Zeolites for Biosensor Applications

There is a considerable attention in the area of electrochemical biosensor modification with various nanomaterials. There are several materials for food quality control and medicine field, such as carbon nanotubes, gold nanoparticles, metal oxides, semiconductors, and zeolites [16].

One of the main focuses on biosensor research is the improvement of performance with long term stability of enzyme electrodes since 1962. There is a considerable interest on modification of biosensor electrodes with various nanomaterials to optimize the enzyme immobilization to increase the response, sensitivity and selectivity. The traditional enzyme immobilization techniques include covalent attachment, entrapment by ion exchange polymers, conducting polymers and cross linking with GA. There are several inorganic alternative candidates for enzyme immobilization such as silica, alumina, glass, and zeolite due to their good mechanical and chemical stability. Zeolites are among the mostly investigated candidates due to their unique ordered pore structures, high surface area and resistance against biodegradation. Electrode modification of the biosensors with zeolites attracted considerable interest to be able to use these unique materials in enzymatic biosensor systems. Even so far, zeolite-enzyme interaction are not fully understood in molecular level, but it is known that these

materials enhance the stability, sensitivity, selectivity, and response time of electrochemical biosensors [17]. It is reported that the molecular sieving selectivity based on size and shape of the guest molecules such as enzymes, charge selectivity and high ion exchange capacity provides an outstanding potential for electrochemical biosensor applications [18]. Also it is possible to determine the effect of one specific parameter with electrochemical biosensors without affecting any other parameters of the zeolites. Soy et al. investigated the effect of heat-treated zeolite Beta crystals on ion-selective field-effect transistors with urea and butyrylcholine chloride. It was observed that zeolite incorporation enhanced enzymatic responses twice for urea and 5 times for butyrylcholinesterase with high reproducibility and stability [19]. Yu et al. reported that zeolite L incorporation onto indium thin oxide glass electrode possess fast electron transfer, broad linear range, low detection limit, long lifetime and stability with cytochrome c [20].

Arvand et al. [21] used mordenite type zeolite to immobilize methylene blue (MB⁺) to form an electron mediator in zeolite modified electrode for amperometric ascorbic acid sensor. It was reported that chemically stable, reproducible, and no pH influence within 2-7 range sensors were utilized.

1.4. Cell Viability

The quantification of cellular growth, with cell proliferation and cell viability is an essential tool for cell based studies. These cell viability measurements enables optimization of cell culture conditions and determine the cell growth factor and cytokine activity. Cell viability measurements assess healthy cells in/on a sample. The viability can be obtained by basically direct counting of cells with the help of an optical microscope but in some specific cases it is impossible to count the cells. In that case, the colorimetric measurements for the healthy cell population by an indicator can be used. An increase in the cell numbers indicates cell growth on samples while a decrease can be explained as a result of toxicity of the sample or inappropriate culture conditions.

Traditional cell viability assays are based on the characteristic parameters of metabolic activity and/or cell membrane integrity of healthy cells. These methods are indirect methods when it compared with counting the cells with the help of a microscope since the metabolic activity of healthy cells measured in cell populations via incubation with a tetra-zolium salt such as MTT ((3-(4,5-Dimethylthiazol-2-yl)-2,5-diphenyltetrazolium bromide), XTT, and etc. which cleaved into colored formazan by metabolic activity of the healthy cells. Mitochondrial MTT reaction is shown in Figure 1.5.

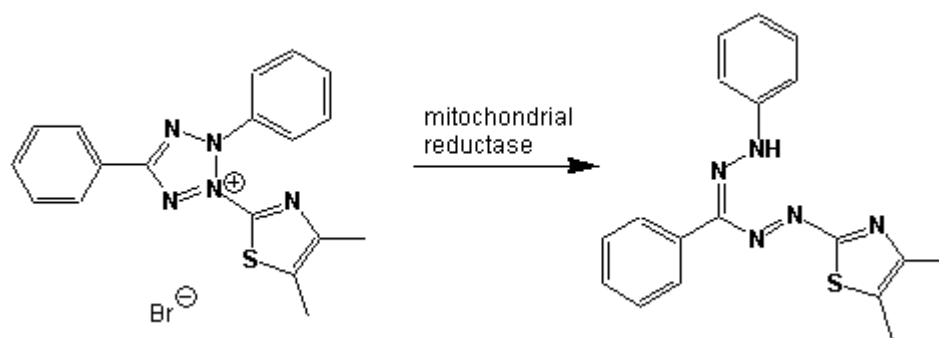


Figure 1.6 Schematic representation of mitochondrial reaction of MTT.

The absorbance of the final products is usually measured with a spectrophotometer while the absorption is dependent on the solvent employed.

CHAPTER 2

LITERATURE REVIEW

Zeolites and zeo-type materials are widely used as microporous materials in various applications such as catalysis, separation processes and molecular sieve applications. Also these crystalline aluminosilicate materials are becoming potential candidates replacing the traditionally used alternatives in biosensor and biomedical applications. The major drawback of using zeolites in such advanced applications is that they are in powder form upon synthesis and this drawback limits the integrating zeolites into device oriented studies. Accordingly, the possibility to attach these particles on solid surfaces to be able to control amount, size and thickness of the zeolite layer is the main challenge to overcome for testing the potential use of zeolites for various applications such as cell adhesion and protein adsorption studies. Accordingly, following literature work is divided into four parts, which are zeolite thin films and forming controlled zeolite patterns on solid substrates, enzyme immobilization and biosensor studies on zeolites, and cell proliferation on zeolites.

2.1 Zeolite Thin Films

Integration of nano and micro particles as well as biomolecules onto different substrates to form ordered crystalline films are of great interest for multipurpose systems in various research areas such as sensors, electronics and biomedical applications [22-27]. The ability of positioning these elements on the finalized system is crucial so that the integrated systems will serve for its designed purpose. The main challenge is to assemble these nanoparticles, which have unique properties, into different compounds for manufacturing advanced devices.

Zeolites are of great interest with their large surface area, tunable surface properties, thermal, chemical and mechanical stabilities with the nanometer scale ordered structure. Furthermore, zeolites show great promise to immobilize biological molecules and potential use in biosensor systems [28-33]. This potential comes from the properties which are readily found in zeolites. The density of the hydroxyl groups on the surface which are important for immobilization applications can be controlled by applying different heat treatment procedures. In this case, the number of defect sites within the zeolites will also alter [34, 35]. Accordingly, other important factors that makes zeolites an important candidate for advanced applications is the sufficient number of surface functional groups ready for further modifications, variable surface hydrophilic/hydrophobic properties, surface charge and high dispersibility in various solutions [36].

In order to make zeolites serve for such advanced components, it is necessary to ensure that they work in harmony with other elements of the system. Although zeolites can be synthesized in a very broad range of surface characteristics and morphologies, which is important for further zeolite dependent applications; the

fact that the synthesized zeolites are in powder form restricts their use in such advanced applications. Thus, it is of increasing interest to organize zeolites in a monolayer on different types of substrates [36-49].

Briefly there are two main approaches used for zeolite formation on solid substrates in literature. The first approach is the well-known secondary growth of zeolites on solid substrates [50, 51]. In this approach, small amount of zeolite crystals, which were synthesized with traditional zeolite synthesis techniques, are seeded onto the surface via dip coating or spin coating methods, and the substrate is placed into the synthesis gel of specific zeolite. Afterwards, the bottle is kept at certain temperature and time in a conventional oven. This approach leads more homogenous and stable film than other approaches, however obtaining desired zeolite film of a particular application can be tricky.

Choi et al. [52] formed MFI zeolite membranes from α and random oriented monolayers with secondary growth of these crystals on α alumina disc support and Wang et al. [53] reported that, it is possible to obtain zeolite MFI monolayers on stainless steel and aluminum alloy with the help of secondary growth methodology and the orientation of the films can be controlled with the orientation of the seed layer of zeolite microcrystals.

Another traditional zeolite thin film production method is simply casting the zeolites on solid substrate with various methodologies such as dip coating, spin coating or direct attachment. The advantages of spin/dip coating approaches are that it is a relatively simple fabrication process and there is no need for using chemicals in this process. Although, it is possible to obtain fully covered surfaces with spin/dip coating methodologies; the uniformity of the films does not meet up the expectations. Hence, direct attachment methodology has the simple production procedure, the full control on coverage rate, and no need for chemical modification for various substrates.

Direct attachment method developed by Prof. Yoon and his group [48] for glass substrates. This method was previously found to be very suitable for the organized assembly of zeolite microcrystals with sizes between 500 nm and 12 μm by Yoon et al. on glass substrates [48].

Lee et al. formed monolayer, double and triple layers of ZSM-5 crystals on glass substrate by direct attachment methodology with the modification of trimethylpropylammonium iodide and sodium butyrate both zeolite and glass substrate. The uniformity, degree of coverage and alignment of zeolite with a perfect closed packed coverage was observed up to three zeolite layers on top of each other [54].

Pham et al. reported that [55] the uniform growth of MFI and BEA zeolite films obtained on substrates with a, b and c oriented crystals while the seed layers prepared with direct attachment methodology for uniform film preparation.

Zhou et al. reported that [49] direct attachment methodology is a facile method for preparing silicalite-1 monolayers on glass substrates supported with polymers such as poly(ethylene oxide) (PEO), poly(vinyl alcohol) (PVA), chitosan, and poly(methyl methacrylate) (PMMA). Also it was reported that the pressure applied during rubbing of the zeolite on substrate affects the formation of monolayer, where pressing hard causes irregular zeolite film while gentle rubbing leads uniform monolayer formation on treated glass substrates.

Öztürk et al. showed that direct attachment method results in a more efficient approach for zeolite assembly on (semi) conductive substrates [56]. It was also reported that it is possible to form zeolite A monolayer with direct attachment methodology on bare un-treated silicon substrates. The surface coverage was 100% in 1 cm^2 area with gentle rubbing and the binding strength of the zeolite

crystals enhanced with baking process right after the monolayer formation in a conventional oven at 120°C for 30 minutes for the first time.

In the present thesis study, direct attachment methodology was also adapted to form zeolite thin films to test their use in cell studies for the first time. This allowed investigating the effect of different type and amount of zeolites for an actual application, which opened the gates of the possibility to use these materials in miniaturized devices in the future.

2.2 Forming Controlled Zeolite Patterns on Solid Substrates

The main challenge of formation of controlled zeolite patterns on solid substrates is the development of new development of sub-micron scale pattern generation method [57]. The difficulties that can be faced during the zeolite pattern formation on substrates are the sensitivity of the chemical linkers to humidity. Most of the linkers need to mixed with dry solvents such as toluene, which tend to dissolve the resist used for generation of patterns in methods like electron beam lithography (EBL) while photolithography and microcontact printing methodologies process that do not necessitate using molecular linkages, are limited to micrometer scale [37, 58]. However, fabrication of smaller sizes needs to be developed which integrates pre-synthesized nanomaterials, in order to meet the demands for high-throughput screening and decreased sample amount [23]. Maximizing the number of assembly sites for biomolecules, and increasing the surface area within the patterns is important for rapid evaluation of biomolecules. Furthermore, a simple and reproducible way, that does not only increase the surface area, but also leads to different activities within each pattern results in controlled selectivity for different molecules with a possible reduction in the

overall array [26]. Thus, a practical method that does not require the use of chemical linkers in order to form nano-micron patterns of organized and uniformly oriented mono and multi layers of zeolite crystals with high degrees of coverage on silicon wafers should be of great interest. For that purpose, there are several approaches suggested in literature. These are simply micro-contact printing, lithographic approaches with secondary growth of zeolites and lithographic approaches with direct attachment of zeolites.

Li. et. al reported that secondary growth on previously patterned and gold coated substrates results preferential growth of silicalite-1 crystals on bare silicon side rather than gold islands [59]. Ha et al. used micro-contact printing method with polydimethylsilane (PDMS) stamp, to build zeolite patterns on silicon wafer [60]. A drop of silicalite-1 suspension drop casted on silicon wafer and patterned PDMS stamp was facedown applied to the wafer with pressure at least 12 hours to evaporate the ethanol and self-assemble the zeolites on wafer.

Öztürk et al. [56] reported for the first time that, zeolite A crystals can be oriented in approximately 250 nm, one zeolite thick lines with the combination of direct attachment method and electron beam lithography on silicon wafer. Also the zeolite layer thickness is fully controlled by the thickness of the electron beam resist [56]. Furthermore, it was also demonstrated that direct attachment leads to a novel and facile approach for creating well organized, fully covered, and strongly bound nano-micron patterns of zeolite A crystals on Si wafer for the first time.

Pellegrino et al. reported the micro-patterning mechanism of silicalite films with etching process [61]. Silicalite crystals were synthesized on silicon wafers. Afterwards photoresist is applied with spin coating and photolithography approach is used. Both dry (ion milling, reactive ion etching) and wet etching

processes applied to the films. In this procedure, it is even applicable to produce zeolite micro cantilevers with high aspect ratios.

Accordingly, direct attachment did not require the use of chemical linkers in order to form nano-micron patterns of organized and uniformly oriented monolayer and multilayers of zeolite crystals with high degrees of coverage on silicon wafers should be of great interest. In the present thesis study, the focus was on investigating a facile and efficient method in order to assemble zeolites for the purpose of generating zeolite nano and micro patterns on the silicon wafer with an extra benefit added, that is the attachment of two different types of zeolites with totally different characteristics on the same solid surface (SiO_2). For that purpose, we again combined “direct attachment” method and electron beam lithography and photolithography techniques for the purpose of assembling zeolite crystals on the silicon wafer.

2.3 Enzyme Immobilization and Biosensor Studies on Zeolites

Enzyme immobilization on zeolites have been of interest for a long time due to the unique properties of zeolite such as the high surface area, controlled hydrophilic/hydrophobic properties, tailorable surface groups, shape, size and charge of the particles. Also the mechanical, chemical, thermal durability and insoluble property in organic solvents, makes these unique crystalline particles an important enzyme immobilization micro-environment [62].

Liu et. al reported a high performance biosensor prepared by the immobilization of glucose oxidase on de-aluminized zeolite Y modified platinum electrode. It is claimed that, high surface area of the zeolite leads high enzyme loading on

electrodes. The modification of the electrode with zeolite resulted high selectivity, long term stability and significantly reduced interference. This performance of the sensor was attributed to the porous structure of the hydrophilic zeolite immobilized matrix which is a favorable microenvironment for enzyme immobilization.

Saiapina et al. reported the modification of conductometric enzyme biosensor modification with natural zeolite clinoptilolite for urea determination. The ion exchange capacity, the ammonium-sieving properties of zeolites and the biological recognition of urease leads a considerable increase in the sensitivity, storage, and operational stability of the sensor.

Layer-by-layer assembly of zeolite Beta and polydiallyldimethyl ammonium (PDDA) for the adsorption of enzymes towards sensitive bio sensing was reported by Zhou et al. It was claimed that, the zeolite film showed amazing adsorption capability for tyrosinase as a model enzyme. The sensor sensitivity found as $400\mu\text{A mM}^{-1}$ and the response reaches 95% of maximum in 5 seconds. The operational and storage stability were found as 2 months [40].

The modification of ion-selective field-effect transistor (ISFET) surfaces with heat treated zeolite Beta crystals for urea and butyrylcholine chloride (BuChCl) determination was reported by Soy et al. It was reported that, the zeolite incorporation enhanced the responses twice for urea and 5 times for BuChCl which attributed to the amount of Brønsted acid sites of the zeolites [19].

2.4. Cell Viability with Zeolites

Several investigations reported that cellular-substrate interactions are associated with the surface topography, chemical composition, surface energy, and surface charge of biomaterials. Zeolites are perspective inorganic nanomaterials for potential biomedical applications due to their unique properties, such as their high surface areas, tunable surface properties, chemical composition, and surface charge with controllable hydrophilic/hydrophobic nature. In literature, the scientists are paying more attention on alternative biomaterials. Zeolite is a candidate for alternative biomaterials with its properties such as biocompatibility, high absorption capacities due to the high surface area with ordered pore structures, high mechanical, chemical, and thermal strength. The researchers are focused on toxicity of these materials on various cells and enzymes. Different zeolite types results various toxicity results on different cell types and enzymes, thus the effects of each zeolite examined individually.

Schütze et. al reported the effects of zeolite A on bone resorbing activity on highly purified avian osteoclasts. It was claimed that, zeolite A can inhibit bone resorption [63]. While Bedi et al. reported zeolite MFI coatings on titanium alloys appears to facilitate osteoblast adhesion and induces osteo-integration. Also the osteo-inductive properties have been enhanced with MFI coating when it compared with bare titanium [8].

It was reported that, zeolite A increases proliferation, differentiation, and transforming growth factor β production in normal adult human osteoblast like cells in-vitro by Keeting et al. The observations indicated that mitogenic action of zeolite A is dependent on initial cell number, which is consistent with the induction of an autocrine factors. Also it is stated that, zeolite A treatment

increases the steady state mRNA levels of the transforming growth factor and induces the release of the latent form of TGF- β protein into the media [64].

Ceyhan et. al reported the crystal structures of various zeolite types were not affected from simulated body fluid (SBF) in 14 days. Furthermore, it is claimed that the silicon amount in the SBF is related with the Si/Al ratio of the zeolite. It was observed that, zeolite A and silicalite were not toxic against myelogenous leukemia and Swiss albino fibroblast culture cells [13].

CHAPTER 3

EXPERIMENTAL

3.1 Synthesis of Zeolites

3.1.1 Synthesis of Zeolite A

Nano sized zeolite A's were hydrothermally synthesized from a mixture having a chemical composition of 11.25 SiO₂ : 1.8 Al₂O₃ : 13.4 (TMA)₂O : 0.6Na₂O : 700 H₂O according to the literature [26]. For the synthesis of zeolite A nanoparticles, tetramethylammonium hydroxide (TMAOH 25%, Sigma Aldrich) and distilled water was stirred for 10 minutes to obtain a homogenous mixture after which aluminum isopropoxide (98%, Acros Organics) was added. Then, the resulting mixture was continuously stirred until it gets transparent (approximately 1 hour). Tetraethyl orthosilicate (TEOS, Acros Organics, 95%) was added as silicon source into the transparent solution and stirred for 30 minutes. Then, previously prepared sodium hydroxide solution (NaOH, J. T. Baker, pellets) was added and the resulting suspension was aged under stirring conditions for 12 hours. After the aging procedure, suspension was placed into a 100°C oven for 8 hours. The solid particles obtained from the synthesis were centrifuged at 13000 rpm, washed with deionized water, and dried at 80 °C.

3.1.2 Synthesis of Zeolite Beta with Varying Si/Al Ratio

Zeolite Beta crystals with Si/Al ratio of 40 and 50 were synthesized with starting gel composition molar formula of $1.92\text{Na}_2\text{O} : \text{Al}_2\text{O}_3 : x\text{SiO}_2 : 4.6(\text{TEA})_2\text{O} : 444\text{H}_2\text{O}$ (where x is 40 and 50) while zeolite Beta with Si/Al ratio of 60 was synthesized with the molar formula of $1.92\text{Na}_2\text{O} : 0.5\text{Al}_2\text{O}_3 : 30\text{SiO}_2 : 4.6(\text{TEA})_2\text{O} : 444\text{H}_2\text{O}$. Sodium aluminate solution was prepared by dissolving sodium aluminate (anhydrous, Riedel de Haen) in a hot solution of sodium hydroxide (J. T. Baker) and deionized water. After cooling to room temperature, tetraethyl ammonium hydroxide (Acros Organics, 20%) was added into the mixture and stirred for 15 minutes at room temperature. Silica containing precursor was prepared by mixing Ludox HS-40 (Sigma-Aldrich) with deionized water. Then alumina and silica sources were mixed and placed in a 140°C oven for 14 days. The solid particles obtained from the synthesis were centrifuged at 13000 rpm, washed with deionized water, and dried at 80°C , overnight.

3.1.3 Synthesis of Silicalite

Silicalite was synthesized with the molar formula of TPAOH: 5TEOS: 500H₂O. Tetraethyl orthosilicate (TEOS, Acros Organics, 95%) was used as the silica source and tetrapropylammoniumhydroxide (TPAOH, Acros Organics, 25%) was used as a template. The mixture of TEOS and TPAOH was continuously stirred for 6 hours at room temperature. The resulting gel was placed in an oven for 18 hours at 125°C . The solid particles obtained from the synthesis were centrifuged at 13000 rpm, washed with deionized water, and dried at 80°C overnight.

3.2 Modification of Zeolites

3.2.1 Ion Exchange of Zeolite Beta with Ag

For the ion-exchange process, 300 mg of zeolite was added into 100 ml distilled water. Calculated amount of Silver Nitrate (AgNO_3 , J.T. Baker), which is approximately 110 mg was added into the zeolite suspension and stirred overnight to change the Na^+ ions to Ag^+ ions. Resulting mixture was filtered and washed with distilled water for 3 times and dried at 80 °C overnight.

3.2.2 Reduction of Ag-ion exchanged Zeolite Beta

For the reduction of Ag^+ ions to Ag^0 , approximately 116 mg of Sodiumborohydride ($\text{NaBH}_4 \geq 98\%$, Merck) was dissolved in 50 ml distilled water and stirred for 10 minutes. Approximately 300 mg of Ag^+ -exchanged zeolite was added into the 50 ml solution and then the obtained solution was slowly stirred until the bubble formation stopped. Resulting suspension was washed three times with distilled water with centrifugation at 10000 rpm for 10 minutes and then dried at 80 °C overnight.

3.2.3 Modification with methyl viologen

In order to modify the zeolite particles with methyl viologen (MV), 100 mg of Methylviologen-dichloride hydrate (98%, Aldrich) was dissolved in 20 mL distilled water and then 300 mg of zeolite was added into the solution. Zeolite and methyl viologen suspension was stirred for 24 hours and resulting suspension was washed three times with distilled water with centrifugation at 10000 rpm for 10 minutes.

3.3 Attachment and Patterning of Zeolites on Solid Substrate

3.3.1 Attachment of Zeolites on Conductometric Biosensor Electrodes

Three different types of electrodes were constructed for this thesis study. General scheme of all electrodes are given in Figure 3.1. The conductometric transducers were produced in Lashkarev Institute of Semiconductor Physics of National Academy of Sciences of Ukraine. They consisted of two identical pairs of gold interdigitated electrodes made by gold vacuum evaporation onto pyroceramic substrate (5 x 40 mm). The surface of sensitive area of each electrode pair was about 1.0 x 1.5 mm. The width of each of interdigital space and digit was 20 μm .

The first type of electrode, which is called as Standard Membrane Transducer (SMT) contains no zeolite and was constructed typically as shown in Figure 3.1 (A). The solution used to prepare the working membrane contains a mixture of 5% urease, 5% BSA, 10% glycerol in phosphate buffer solution (PBS), while the solution used to prepare the reference membrane contains a mixture of 10% BSA, and 10% glycerol. Then transducers exposure to GA vapor for 35 minutes.

The second type of electrode, which is called as Zeolite Membrane Transducer (ZMT) contains zeolite particles that were simply added to the immobilization mixture as shown in Figure 3.1 (B). Accordingly, the solution used to prepare the working membrane contains a mixture of 5% zeolite, 5% urease, %5 BSA, 10% glycerol in PBS, while a mixture of 5% zeolite, 10% BSA, and 10% glycerol in PBS without any enzyme was used for the reference membrane. Then transducers exposure to GA vapor for 35 minutes.

The third and the final type of electrode was called as Zeolite Coated Transducer (ZCT) and was developed from zeolite thin films prepared on gold electrodes of conductometric biosensors as shown in Figure 3.1 (C). The transducer surfaces of both working and reference electrodes were modified by dip coating the surfaces with 5% zeolite suspension. Then 0.1 μ l, 5% urease solution in PBS was dropped on the working electrode side and 0.1 μ l, 5% BSA in PBS was dropped on the reference electrode side of the electrode. The electrodes were not kept under GA vapor for this modification route.

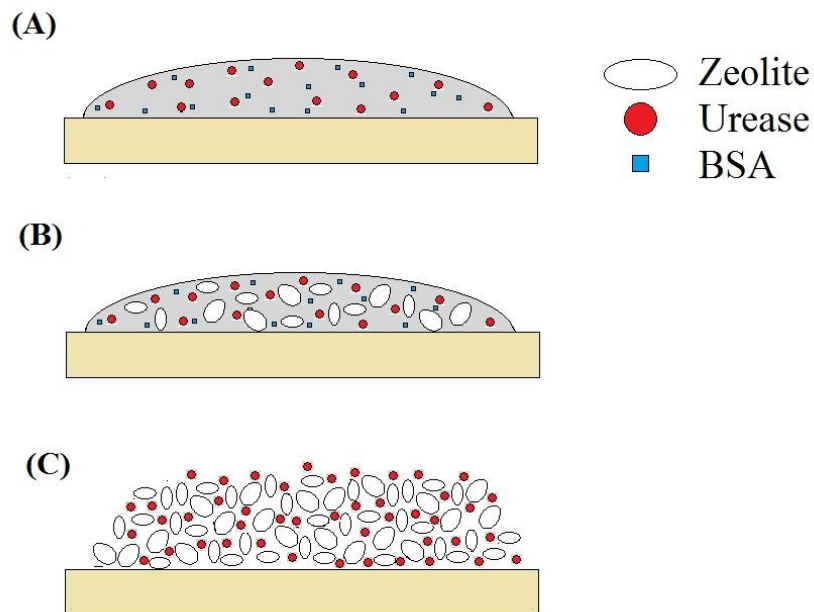


Figure 3.1 Schematic representation of electrodes; (A) Standard Membrane Transducer (SMT), (B) Zeolite – Membrane Transducer (ZMT), (C) Zeolite Coated Transducer (ZCT).

3.3.2 Attachment of Zeolites on Silicon Surfaces

According to the literature studies [46, 47, 56], direct attachment methodology is used to perform the attachment of zeolite A and silicalites on silicon surfaces. Silicon wafers were cut into small pieces and placed on an aluminum foil. Proper amount of zeolite powder was put on the surfaces and they were gently rubbed onto the surfaces by a finger. The coverage and topography can be examined by using a light microscope during this procedure. After the optimum attachment level, zeolite coated surfaces placed in a conventional oven for 30 minutes.

3.3.3 Zeolite Patterning with Electron Beam Lithography

3.5 wt. % diluted polymethylmetacrylate (PMMA 7%, Microchemicals) in chlorobenzene was spin coated on silicon wafer pieces with 6000 rpm for 40 seconds and resulting resist thickness was approximately 400 nm. The coated wafers pre-baked at 160 °C for 30 minutes. Patterns that already programmed were utilized by Electron Beam Lithography system (EBL, Xenos XeDraw2 Pattern Generator attached to CamScan CS300 SEM). Patterned surfaces were developed by methylisobutylketone/isopropanol (MIBK/IPA, 1/1) solution for 30 seconds, rinsed with IPA, washed with distilled water and dried with N₂ gas flow. Direct attachment method, which is already found as the most efficient procedure for zeolite attachment by Öztürk et al. [56] was applied to the patterned surfaces. The coverage and topography can be examined by using a light microscope during this procedure. After the optimum attachment level, zeolite coated surfaces placed in a conventional oven for 30 minutes. Surfaces were rinsed with acetone, washed with distilled water and dried with N₂ gas flow. Coverage of the patterned areas was examined by Scanning Electron Microscope (SEM). Schematic representation of the procedure can be seen in Figure 3.2.

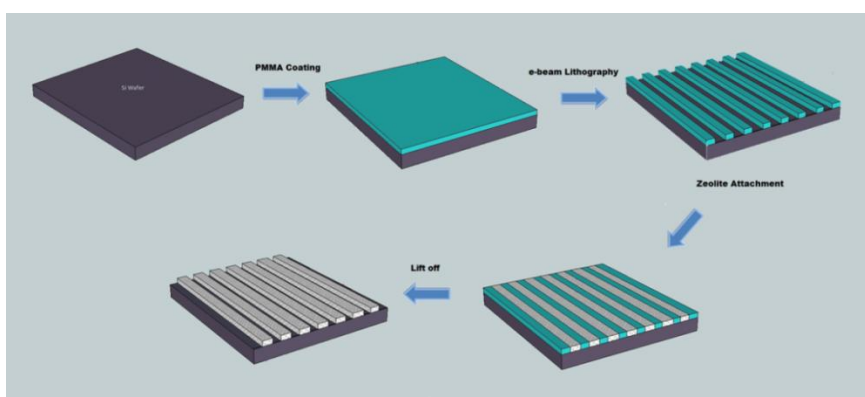


Figure 3.2 Schematic representation of zeolite patterning procedure with EBL.

In addition to this, full combination of direct attachment method and e-beam lithography was used in the same procedure to obtain zeolite patterns on another zeolite layer, which was already attached on silicon surface. Schematic representation of this procedure can be seen in Figure 3.3.

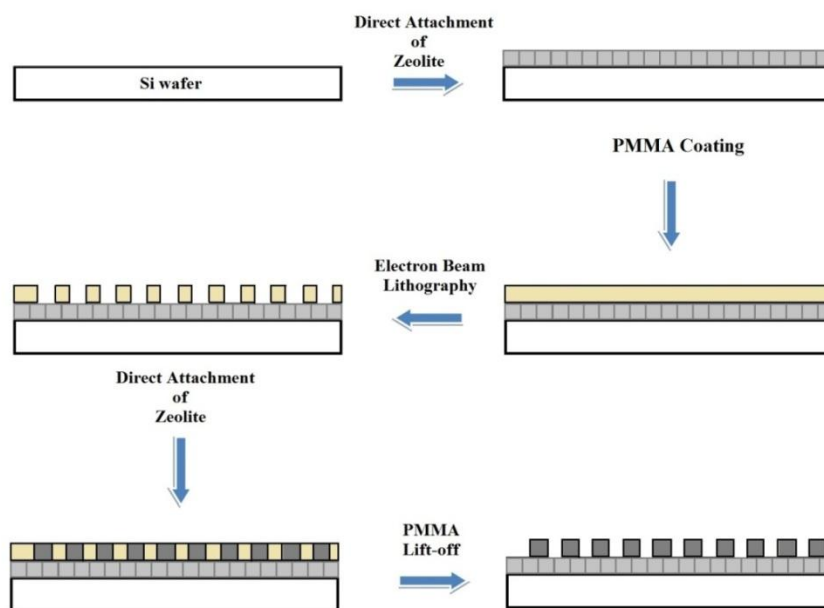


Figure 3.3 Schematic representation of zeolite patterning procedure on top of a zeolite monolayer with EBL.

3.3.4 Zeolite Patterning with Photolithography

AZ 5214 photoresist (Microchemicals) was spin coated on silicon wafer pieces with 6000 rpm for 40 seconds and resulting resist thickness was approximately 1 μm . The coated wafers pre-baked at 110 $^{\circ}\text{C}$ for a minute. Masks that were already

prepared previously with Heidelberg Instruments, DWL-66 model mask writer at UNAM, Bilkent University, were aligned and utilized by photolithography system at GÜNAM, METU. Patterned surfaces were developed by AZ 726 (Microchemicals) metal ion free developer solution for approximately 10 seconds, rinsed and washed with distilled water and dried with N₂ gas flow. Direct attachment methodology was applied to the patterned surfaces, with the same manner explained in Zeolite Patterning with Electron Beam Lithography section (Section 3.3.3). Schematic representation of the procedure can be seen in Figure 3.4.

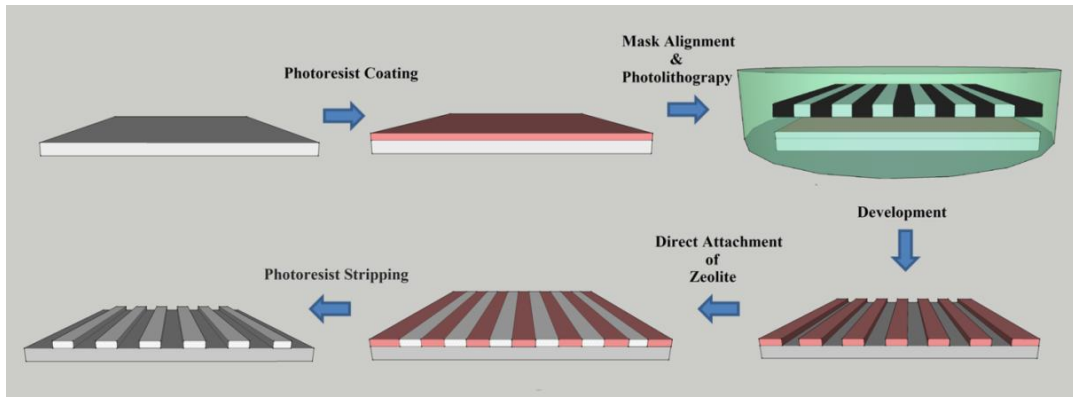


Figure 3.4 Schematic representation of zeolite patterning procedure with PL.

Also the full combination of direct attachment method and PL can be used in the same procedure to obtain zeolite patterns on another zeolite layer already attached on silicon surface. Schematic representation of this procedure can be seen in Figure 3.5.

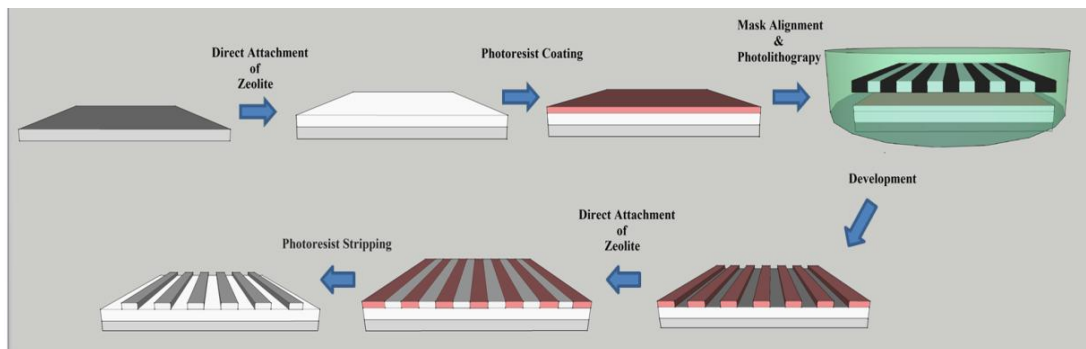


Figure 3.5 Schematic representation of zeolite patterning procedure on top of a zeolite monolayer with PL.

3.4 Cell Viability Measurements

3.4.1 MTT assays with MG63 Cell Lines

Cell proliferation was assessed by monitoring the conversion of MTT to formazan. The reduction of MTT is catalyzed by mitochondrial dehydrogenase enzymes and is therefore a measure for cell viability.

MTT assays were performed after 24, 48, and 72 hours of incubation. MG63 osteoblast like cells are seeded on surfaces on 24 well culture plates with 2×10^4 cell/well in 800 μ l media. 10 μ l of MTT (3-[4, 5-dimethylthiazol-2-yl]-2, 5-diphenyltetrazolium bromide) at a concentration of 5 mg/ml in PBS was added to each well after 24, 48, and 72 hours of incubation respectively. The plates were then incubated at 37 °C in 5% CO₂ for 4 hours. The samples do not cover

the bottom of the 24 well plates, for that reason, some cells will adhere to remaining well surface. To get realistic results from the samples, just before DMSO process, samples taken out from the original 24 well plate and placed in a new 24 well plate, which already prepared with 100 μ l DMSO inside. Also the medium at the original 24 well plate removed and 100 μ l DMSO added each well and formazan solubilized. After solubilization of formazan, absorbance was read immediately using a spectrophotometer at 570 nm.

3.4.2 MTT assays with NIH3T3 Cell Lines

MTT assays were performed after 24, 48, and 72 hours of incubation. NIH 3T3 fibroblast cells were seeded on surfaces on 24 well culture plates with 2×10^4 cell/well in 800 μ l media to get comparable results with MG63 cell line experiments. The same MTT assay applied to NIH 3T3 cells.

3.5 Material Characterization

3.5.1 X-Ray Diffraction (XRD)

X-Ray diffraction (XRD) analysis was done by Ni filtered Cu-K α radiation (Philips PW 1729) with zeolite A, zeolite Beta and silicalite particles for phase identification. The voltage was 40 kV and current was 30 mA during the experiments. The diffraction peaks were scanned between 5-40 $^\circ$ 2 θ degrees with

step size of 0.03° and $0.1^\circ/\text{s}$. Time constant was 1s, and slit was 0.2 mm. These measurements were performed at Central Laboratory, METU.

3.5.2 Scanning Electron Microscopy (SEM)

The scanning electron microscopy images of zeolite A, zeolite Beta, silicalite and the zeolite patterns were collected with 400 Quanta FEI model FE-SEM with various accelerating voltages and beam currents. These measurements were performed at Central Laboratory, METU.

3.5.3 Particle Size Analysis

Particle size analysis of zeolite Beta particles with varying Si/Al ratios was done by Aerosizer Time of Flight particle size analyzer. These measurements were done at CAMMP laboratory, Northeastern University, MA, USA.

3.5.4 Contact Angle Measurements

The wettability of the silicalite and zeolite A monolayer coated film surfaces was monitored by determining the contact angle of a 1- μL deionized water droplet using a video contact angle measuring system (VCA 2500, AST, Billerica, MA).

These measurements were done at Department of Biomedical Engineering, McGill University, QC, Canada.

3.5.5. Pore Size Distribution

To determine the physical characteristics of each material, nitrogen adsorption–desorption isotherms were measured at 77 K on a Quantachrome Corporation, Autosorb-6. The zeolites were degassed at 300 °C under high vacuum for 4 hours prior to the nitrogen adsorption measurements. The average pore size was taken as the peak of the pore size distributions as calculated from the adsorption branch using the Barrett-Joyner-Halenda (BJH) method. The total pore volume was determined as the volume of liquid nitrogen adsorbed at P/P_0 of 0.995. These measurements were performed at Central Laboratory, METU.

3.6 Conductometric Biosensor Measurements

The electrochemical measurements were performed with an electrochemical device (Stanford Research Systems Model SR830 Lock-In Amplifier) connected to a PC through the serial port. All of the experiments were carried out using a 5 mL beaker filled with 5 mM PBS of pH 7.2. The substrate (Urea) added is 1 mM in each reading. Every experiment was repeated for 5 times.

CHAPTER 4

RESULTS AND DISCUSSION

4.1 Synthesis, Characterization and Modification of Zeolite and Zeo-type Materials

4.1.1 Zeolite A

Zeolite A crystals were hydrothermally synthesized from a mixture having a chemical composition as 11.25 SiO₂ : 1.8 Al₂O₃ : 13.4 (TMA)₂O : 0.6Na₂O : 700 H₂O. The XRD diffractograms of the synthesized zeolite A crystals are shown in Figure 4.1. The typical peak positions of zeolite A were observed in the synthesized ones as well. Accordingly, all of the synthesized ones matched the data reported in literature (Appendix A) and thus indicated that the products were pure material.

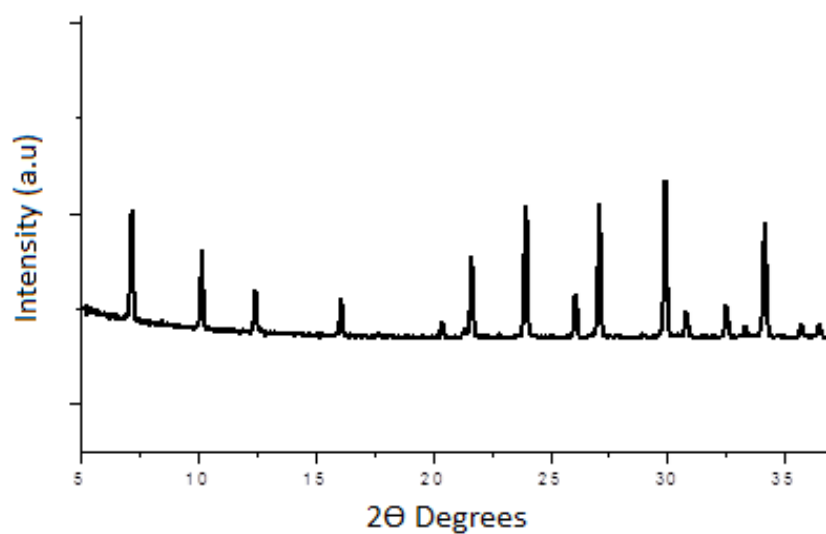


Figure 4.1 XRD diffractograms of the synthesized zeolite A particles.

Scanning electron microscopy images of the synthesized zeolites are given in Figure 4.2. Particle sizes are approximately in the range of 0.2-0.3 μm . All particles possess the characteristic cubic like shape of as observed in the micrographs with slightly truncated edges.

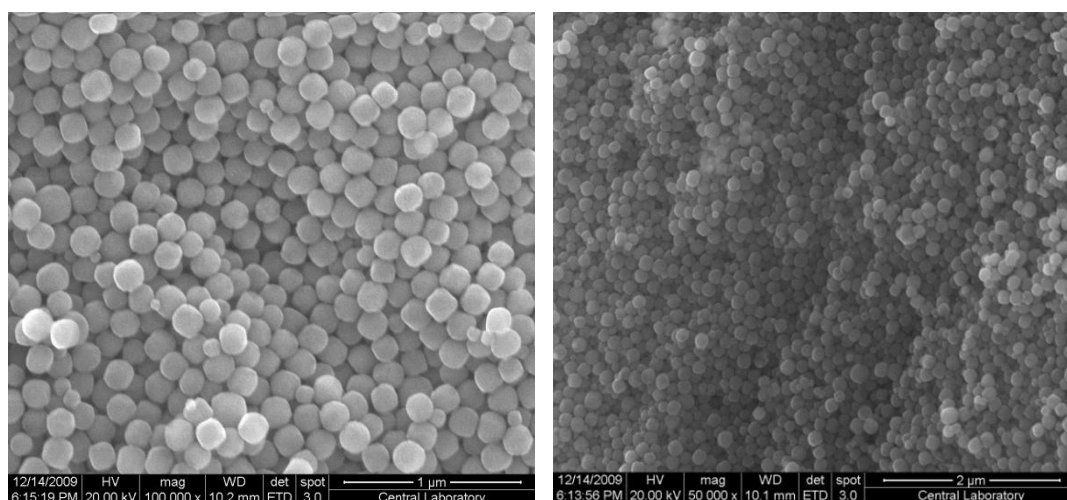


Figure 4.2 Scanning electron microscopy images of zeolite A particles with different magnifications.

4.1.2 Zeolite Beta with Varying Si/Al Ratio

Crystals of zeolite Beta with Si/Al ratio of 40 and 50 were hydrothermally synthesized from a gel with the molar formula of $1.92\text{Na}_2\text{O} : \text{Al}_2\text{O}_3 : x\text{SiO}_2 : 4.6(\text{TEA})_2\text{O} : 444\text{H}_2\text{O}$ (where x is 40 and 50) and Si/Al ratio of 60 synthesized with the molar formula of $1.92\text{Na}_2\text{O} : 0.5\text{Al}_2\text{O}_3 : 30\text{SiO}_2 : 4.6(\text{TEA})_2\text{O} : 444\text{H}_2\text{O}$. The XRD diffractograms of the synthesized zeolite Beta crystals are shown in Figure 4.3 and compared with the literature (Appendix A). The typical peaks of zeolite Beta samples were observed in the synthesized ones as well. Accordingly, all of the synthesized ones matched the data reported in literature and thus indicated that the products were pure material.

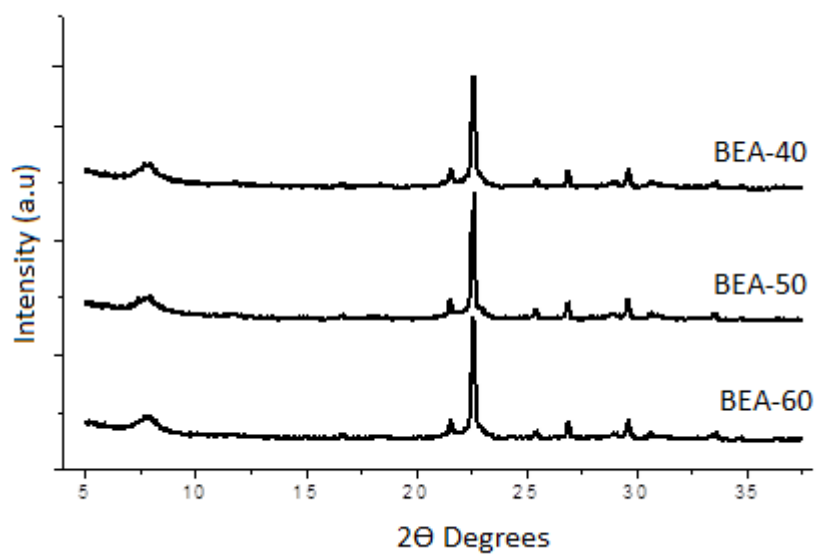


Figure 4.3 XRD diffractograms of the synthesized zeolite Beta particles.

Scanning electron microscopy images of the synthesized zeolites are given in Figure 4.4 and the properties of the synthesized zeolites are given in Table 4.1.

Table 4.1 Surface properties of zeolite Beta crystals.

Materials	Si/Al ratio ^a	S _{BET} (m ² /g) ^b	Particle size (μm) ^c	Pore size (Å) ^d	Pore volume (cc/g) ^d
BEA40	12.9	349	0.79	10.01	1.46
BEA50	21.2	462.2	0.83	9.46	1.93
BEA60	24.5	376.1	0.91	10.45	1.53

^a Measured by EDX.

^b Measured by BET.

^c Measured by API Aerosizer LD.

^d Measured by SF Method.

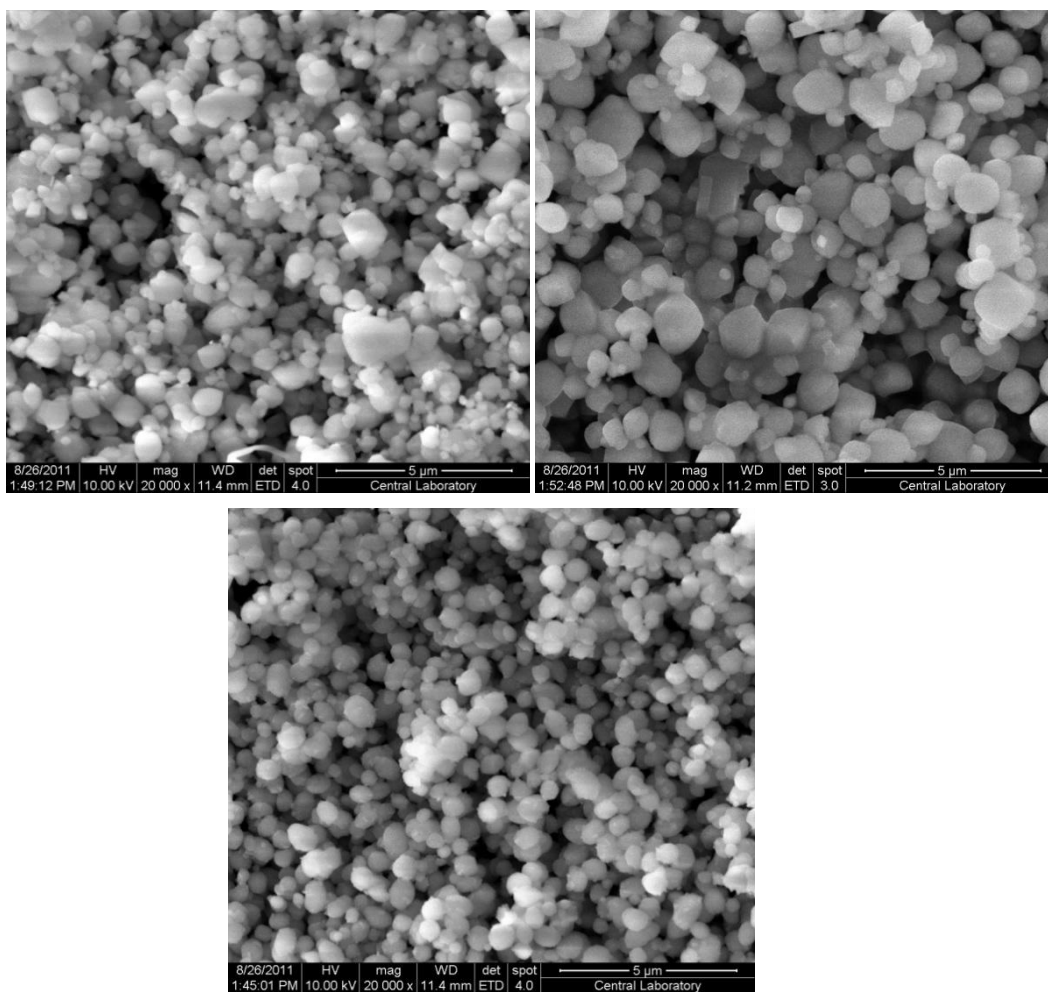


Figure 4.4 Scanning electron microscopy images of zeolite Beta's with Si/Al ratio of 40 (A), 50 (B) and 60 (C).

4.1.3 Silicalite

Silicalite have been of great interest in biological studies for their pure silica nature and thus the leading hydrophobic properties. Silicalite particles were synthesized with the molar formula of TPAOH: 5TEOS: 500H₂O. The XRD diffractograms of the synthesized silicalite crystals are shown in Figure 4.5. The typical peak positions of silicalites were observed in the synthesized ones as well. Accordingly, all of the synthesized ones matched the data reported in literature (Appendix A) and thus indicated that the products were pure material.

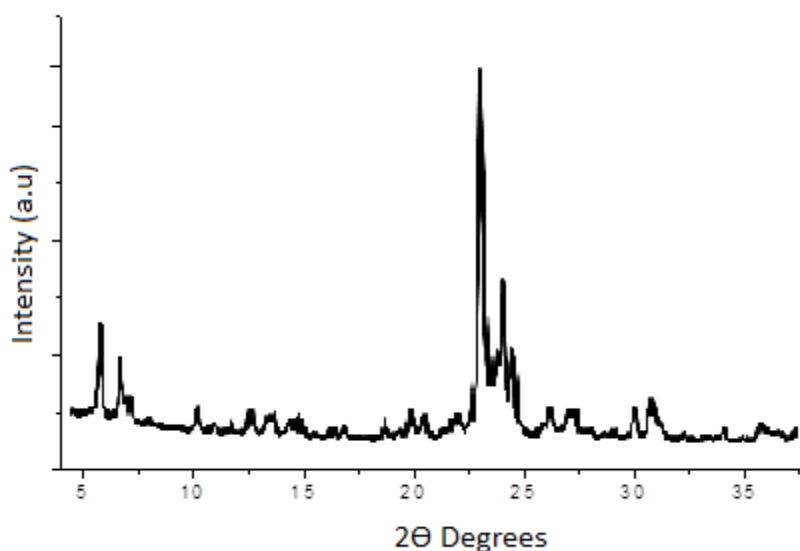


Figure 4.5 XRD diffractograms of the synthesized silicalite particles.

The surface area of these silicalite crystals determined as 281.7 m²/g with BET and pore size were determined as 4.26 Å while pore volume found as 3.61 cc/g with SF method. The particle size found as approximately 0.5 μm with API Aerosizer LD.

Also the particles examined by scanning electron microscope to get information about the morphology and particle sizes. Scanning electron microscopy images of the synthesized zeolites are shown in Figure 4.6. Particle sizes are approximately in the range of 0.5 μm and the particles have the unique plate-like silicalite shapes.

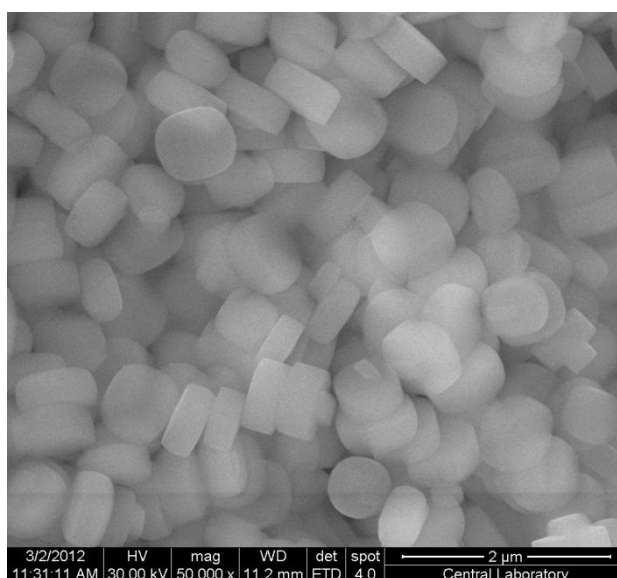


Figure 4.6 Scanning electron microscopy images of silicalite particles.

4.2 Modification of Zeolites with Silver and Methylviologen

For ion-exchange studies, zeolite Beta was chosen as the zeolite type due to its high Si/Al ratio range unlike any others. Zeolite Beta has a framework structure of three dimensional networks of 12-ring channels. This property of zeolite Beta makes it a good candidate for investigating the effect of ion-exchange on conductometric biosensor systems. Accordingly, Na^+ ions in zeolite Beta were ion exchanged with Ag^+ and then were subjected to reduction to make Ag^0 -Zeolite Beta particles. Also the same zeolites were modified with MV^+ to investigate the effect of MV on conductivity change in the zeolite during the conductometric measurements. Zeolite Beta in as-prepared and ion-exchanged forms has been characterized using EDX.

Table 4.2 Properties of ion exchanged sub-micron zeolite Beta crystals.

Sample Name	Na (at.%)	Ag (at.%)	C (at.%)
Zeolite Beta 40	0.4	-	-
Ag ⁺ Beta 40	0.05	0.27	-
Ag ⁰ Beta 40	0.37	0.13	-
MV Beta 40	0.06	-	0.15
Zeolite Beta 50	0.27	-	-
Ag ⁺ Beta 50	0.05	0.24	-
Ag ⁰ Beta 50	0.15	0.13	-
MV Beta 50	0.1	-	0.3
Zeolite Beta 60	0.26	-	-
Ag ⁺ Beta 60	0.04	0.16	-
Ag ⁰ Beta 60	0.14	0.25	-
MV Beta 60	0.06	-	0.4

4.3 Zeolite Attachment and Patterning

4.3.1 Attachment of Zeolites on Conductometric Biosensor Electrodes

After the synthesis of different types of zeolites, next goal was to attach these zeolites in powder form on different substrates to be able to investigate their influence on biosensor measurements. There are several methods for zeolite attachment on solid substrates such as spin coating, dip coating and direct attachment [59]. For the current study, dip coating of zeolite on conductometric electrode surfaces was chosen, because the shape of the electrodes are not suitable

for spin coating or direct attachment methods. Furthermore, gold lines in interdigitated part of the electrodes are highly sensitive to rubbing zeolite particles on the electrodes in direct attachment methodology. Figure 4.7 displays the scanning electron microscopy images of a typical zeolite coated conductometric biosensor electrode upon modifying the electrode surface with silicalite and zeolite Beta particles.

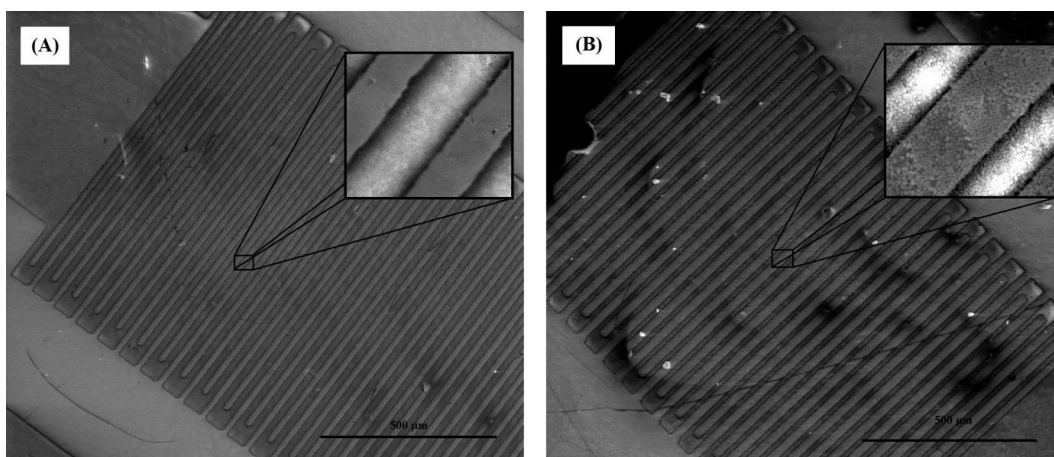


Figure 4.7 Scanning Electron Microscopy images of the Zeolite Coated Transducers (ZCT) with Silicalite (A) and Zeolite Beta Si/Al ratio of 60 (B).

4.3.2 Attachment of Zeolites on Silicon Substrates

With all the amazing properties of zeolites, the only disadvantage of this material is the powder form and attachment of these zeolites on solid substrates is an important field to overcome this problem. There are several methodologies to attach these particles on substrates discussed above, direct attachment was chosen

for silicon substrates, because it was found that this method provides uniform distribution on substrate and it is easy to build them [59].

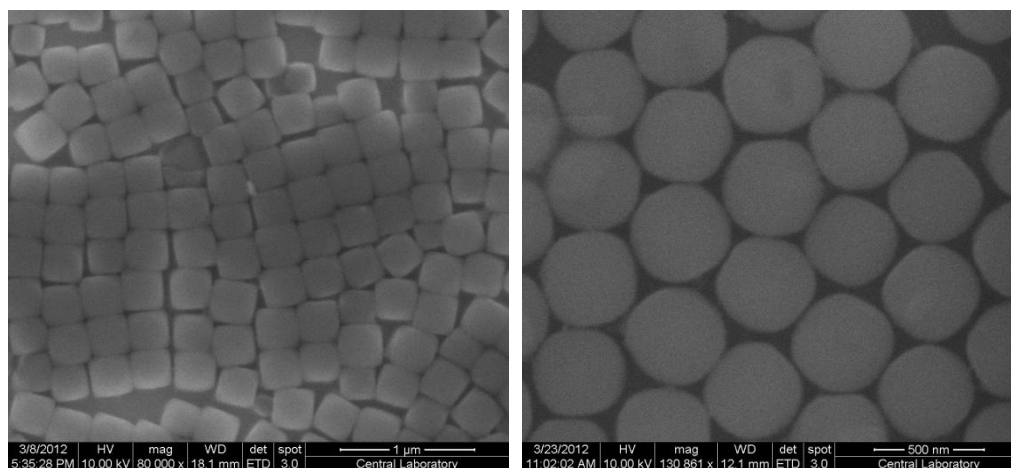


Figure 4.8 Scanning electron microscopy images of s of zeolite A (A) and silicalite (B) monolayers formed by direct attachment on silicon substrate.

Very large surface area is one of the most important properties of zeolitic materials and attachment of these particles on solid substrates may lead the use of these zeolites in various applications. Also for every different application, the modification of these zeolites with various chemicals can form several different surface groups such as $-\text{NH}_4$, $-\text{CH}_4$ or $-\text{H}^+$ instead of $-\text{OH}$. Since the properties of these zeolites are different from each other, the surface properties of the samples prepared with different zeolites will vary. The contact angle measurements of zeolite A and silicalite monolayers were given in table 4.3.

Table 4.3 The Contact Angle Measurements of zeolite monolayers

Sample name	Contact Angle (degrees)
Zeolite A monolayer	71.35 ± 3.07
Silicalite monolayer	89.35 ± 4.03

4.3.3 Zeolite Patterning with Electron Beam Lithography

The combination of direct attachment method and e-beam lithography leads full control on patterns with both width, height in nanometer level of resolution, and coverage of the zeolite coated areas. For this purpose, various different lithographic patterns were successfully fabricated using silicalite, which has higher hydrophobicity and zeolite A, which is more hydrophilic (Section 4.3.2). Scanning electron microscopy images of these patterns are shown in figure 4.9.

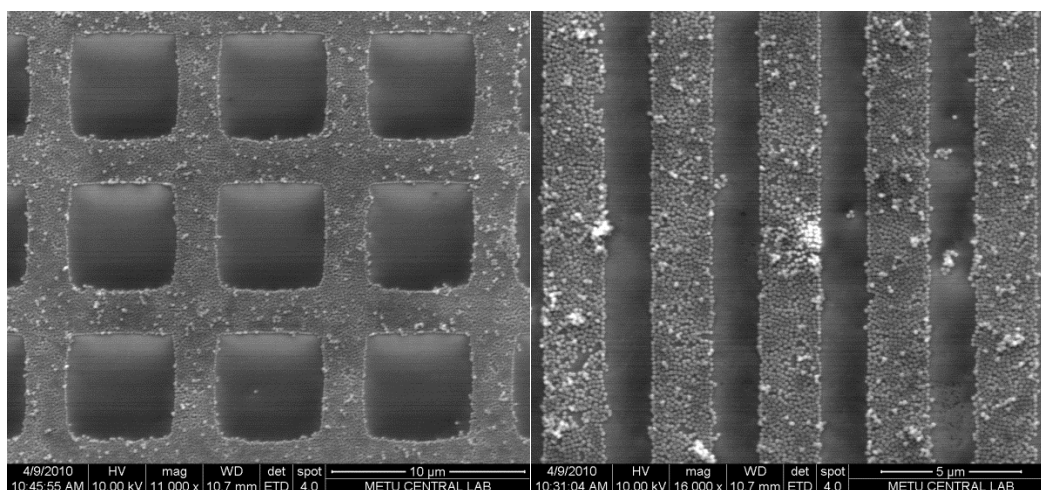


Figure 4.9 Scanning electron microscopy images of zeolite A monolayer patterns formed by EBL.

In that way, it was possible to obtain nano-sized patterns in full control. However, total area of the patterns can only be in micrometer scale due to high patterning time and lack of electron beam stability.

The fabrication of zeolites and zeo-type material patterns with micrometer and nanometer scale regularity on several solid substrates might be a good alternative candidate for several bio-applications with increased surface sites and full control on the surface. Accordingly, two different types of zeolites, silicalite and zeolite A, with varying surface properties were successfully fabricated on the same silicon substrate with a control of zeolite pattern sizes ranging from 500 nm to 5 μm by direct attachment methodology. This method allowed one to have a better control on differentiated areas on sample. For this purpose, various patterns were fabricated, where silicalite line patterns were formed on zeolite A monolayer and zeolite A line patterns were formed on silicalite monolayer for the first time. Scanning electron microscopy images of these patterns are shown in Figure 4.10.

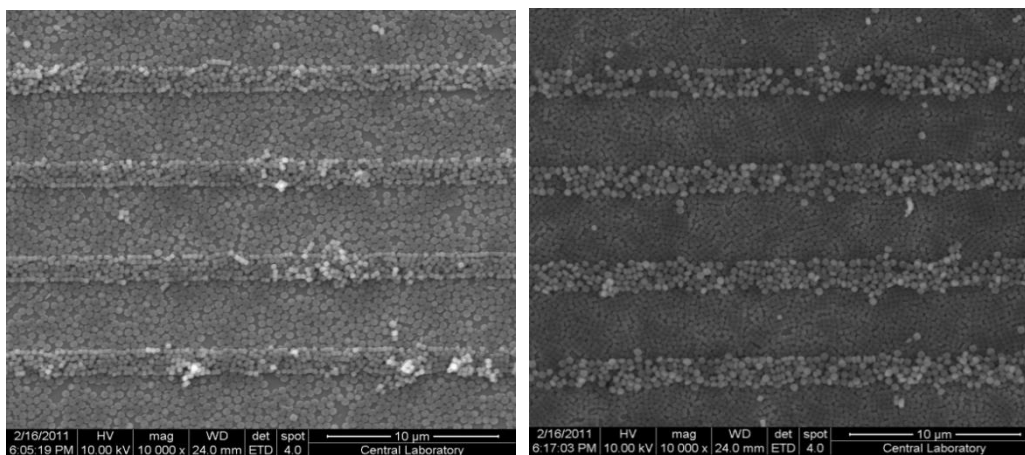


Figure 4.10 Scanning electron microscopy images of zeolite A line patterns on silicalite monolayer (A) and silicalite line patterns on zeolite A monolayers (B) formed by EBL.

4.3.4 Zeolite Patterning with Photolithography

The combination of direct attachment method and photolithography was believed to result in full control on the size of zeolite patterns, leading to changing the pitch within micron size resolution and coverage. For this purpose, various patterns were applied using silicalite and zeolite A and scanning electron microscopy images of two zeolite patterned substrates with pitch lengths of 20 μm and 60 μm are shown in Figure 4.11.

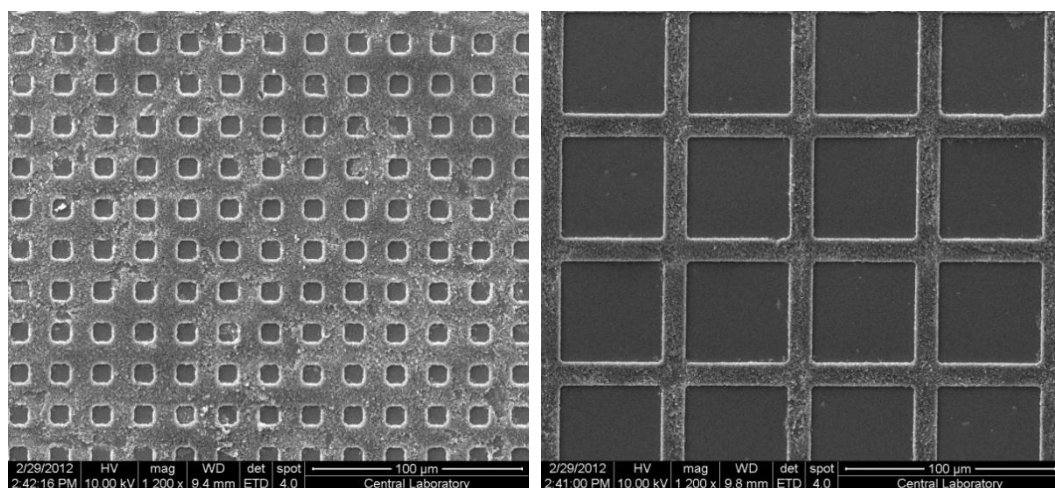


Figure 4.11 Scanning electron microscopy images of two different zeolite A pattern formations prepared with PL.

These studies showed that using electron beam lithography for making zeolite patterns on silicon substrates was more convenient to form micrometer sized patterns (500 nm to 10 μm pitches) however the total patterned area cannot be in centimeter scale because it will take days and hours to pattern that much area. If

one aims to make zeolite patterns of centimeter scale, photolithographic approach would be more suitable. Biggest advantage of the photolithography system is the time spent for lithography. It would be possible to pattern the whole silicon wafer substrate in just a couple of seconds using photolithographic approach.

Accordingly, direct attachment method to attach zeolite particles was combined with photolithography in a similar fashion with the electron beam approach in order to fabricate two different types of zeolites on the same surface. In this way, it was easier to form controlled differentiated areas on a single silicon surface. Representative figures showing scanning electron microscopy images of the zeolite patterns obtained after combining direct attachment and photolithography are shown in Figure 4.12.

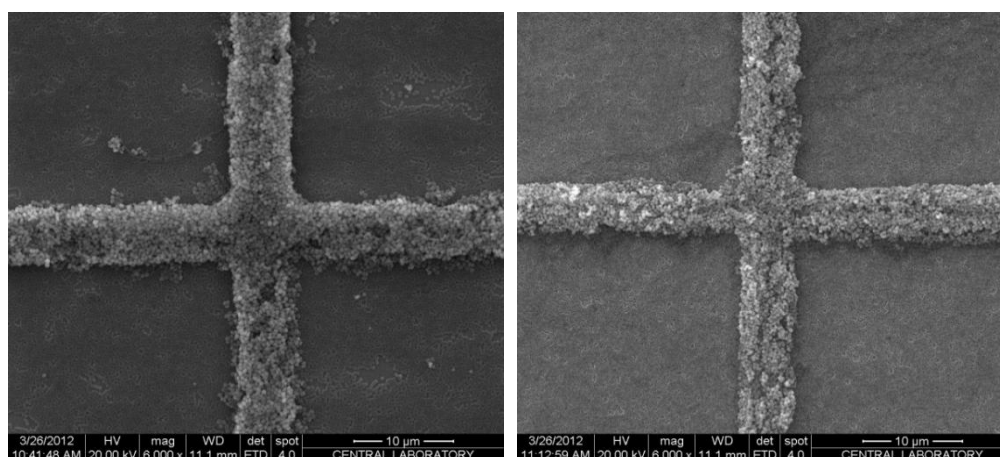


Figure 4.12 Scanning electron microscopy images of zeolite A cross-line patterns on silicalite monolayer (A) and silicalite cross-line patterns on zeolite A monolayer (B) formed by PL.

Electron beam lithography leads smaller feature size for zeolite patterning applications with achieved minimum line width of 250 nm [56], but the maximum

patterned area is limited with the electron beam stability in long time patterning. Even the total patterning ability of electron beam lithography just limited with sample holder of the system, this electron beam stability problem with increasing time increases and it results worse pattern generation. This is not the only disadvantage of that system since the very long time of large scale patterning. It takes days and hours for centimeter level of patterning area with electron beam lithography systems. To overcome these problems, photolithography technique is used. It just takes a couple of seconds to generate the patterns on whole 3” silicon wafers and the pattern success is the same in every single point in the patterns, but in this approach, mask is the limiting parameter for minimum feature size. The minimum feature size is 1 μm with the accessible infrastructures in mask production, but in this case, minimum pattern widths were chosen as 5 μm . Also another challenge is the thickness of the photoresist film. It is almost impossible to obtain single layer of zeolite thick patterns, since the form of the photoresist is a lot more viscous than electron beam resist. Some representative zeolite patterns generated can be seen in Appendix B.

4.4 Cell Viability Measurements

The fabrications of zeolites on solid substrates were achieved with electron beam lithography and photolithography systems with various pitches and total patterned areas. These pattern properties and zeolite type is the main parameter of the surface properties of these samples. Since surface properties of the samples are one of the deterministic parameter for cell adhesion studies, it is expected to vary the cell adhesion behavior from sample to sample.

Accordingly, the effect of the fabrication of zeolite patterns on cell behavior was studied by using the zeolite fabricated substrates with photolithography. The ones fabricated using electron beam lithography were not used, since the patterns formed by this method were too small for such cell studies. Also, it takes a lot of time and money to obtain enough samples for biological applications.

4.4.1 MTT assays with MG63 Cell Lines

Cell proliferation is assessed by monitoring the conversion of MTT to formazan. The reduction of MTT is catalyzed by mitochondrial dehydrogenase enzymes and is therefore a measure for cell viability. MTT assay results these samples with MG63 cells in 24, 48, and 72 hours of incubation times were given in Figure 4.13, 4.14, and 4.15.

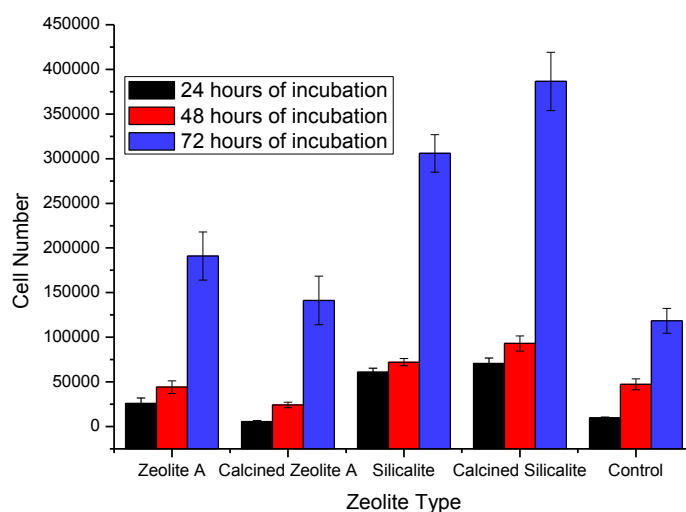


Figure 4.13 MTT assay results for various samples after 24, 48, and 72 hours of incubation for MG63 Cell Line with 0.125 cm^2 zeolite coated samples.

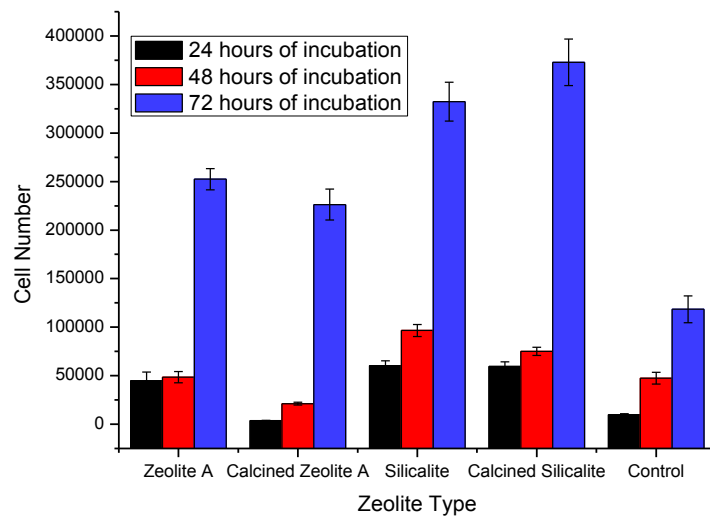


Figure 4.14 MTT assay results for various samples after 24, 48, and 72 hours of incubation for MG63 Cell Line with 0.08825 cm² zeolite coated samples.

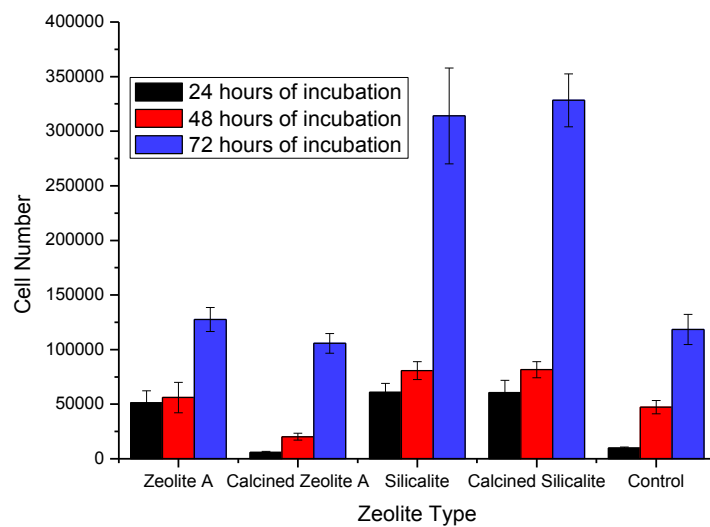


Figure 4.15 MTT assay results for various samples after 24, 48, and 72 hours of incubation for MG63 Cell Line with 0.04167 cm² zeolite coated samples.

Figure 4.13, 4.14, and 4.15 showed that silicalite coated samples has higher amount of cells than zeolite A coated samples after 24, 48 and 72 hours of incubation. This may be referred to the hydrophilic/hydrophobic properties, surface charge, and/or particle size of zeolites. Thian et al. reported that more hydrophilic and negatively charged surfaces enhance the attachment, proliferation and differentiation of cells [65]. In this case, zeolites with lower hydrophilicity and positive charge showed higher proliferation with MG63 cell lines, which may be affected from cell type and also the surface area effect of the highly porous zeolites. That's why, the effect of zeolite amount on samples were examined and compared. Patterned area on the samples refers the zeolite amount and it can be seen from Figure 4.16, 4.17 and 4.18 that increasing zeolite amount leads higher cell numbers in these sample sets. MTT assay results of MG63 cells in the control group and the zeolite patterned surfaces can be seen in Figure 4.16, 4.17, and 4.18.

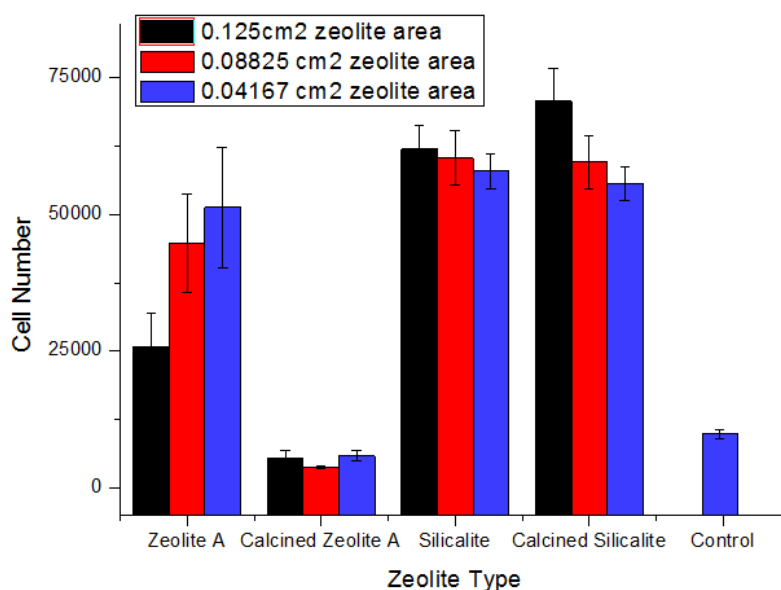


Figure 4.16 MTT assay results for various samples with 0.125, 0.08825, and 0.04167 cm² zeolite patterned area for MG63 Cell Line for 24 hours incubation.

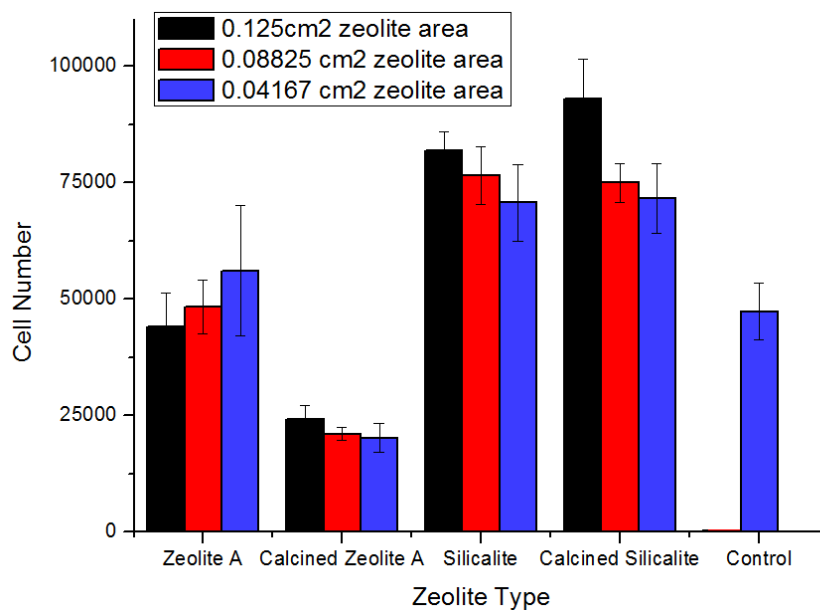


Figure 4.17 MTT assay results for various samples with 0.125, 0.08825, and 0.04167 cm² zeolite patterned area for MG63 Cell Line for 48 hours incubation.

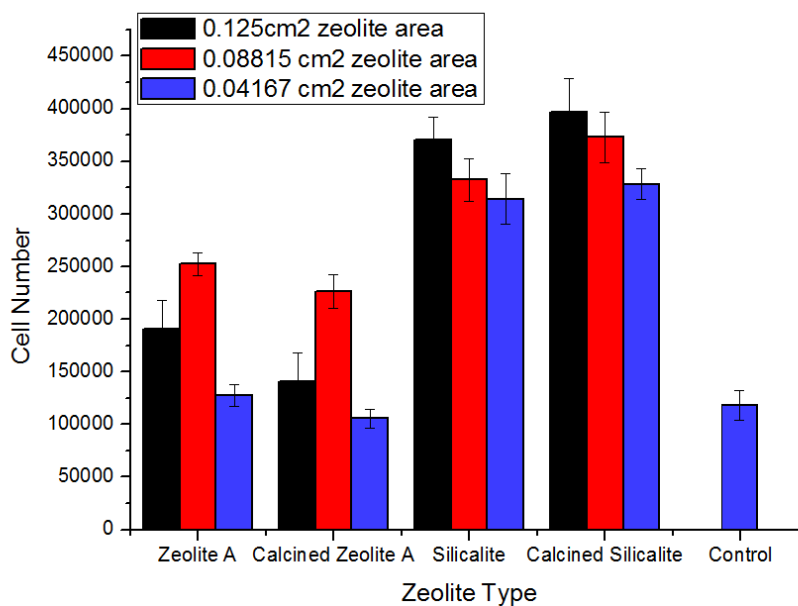


Figure 4.18 MTT assay results for various samples with 0.125, 0.08825, and 0.04167 cm² zeolite patterned area for MG63 Cell Line for 72 hours incubation.

According to Figures 4.16, 4.17, and 4.18, when silicate particles were used to pattern the silicon surfaces, increasing amount of zeolite resulted in an increase in the number of cells attached onto these surfaces after 24, 48, and 72 hours of incubation. Statistical analysis confirmed that there is a significant difference between 0.04167cm² silicalite coated samples and 0.125 cm² silicalite coated samples after 48 hours of incubation (p=0.03) while there is no significant difference between these samples after 24 and 72 hours of incubation (p=0.33 and 0.34 respectively). Higher zeolite amount on the samples leads higher surface area on each sample which showed more proliferation on these samples. It shows that, cells not only adhere and proliferate on the bare silicon surfaces, but also on the zeolite coated areas. Fenoglio et. al reported that the increase in the amount of porosils (pure silica materials), decreased the total number of cells with macrophages [66]. However Keeting et al. [64] claimed that zeolite A increase the proliferation of osteoblast cells, similar to the obtained results. It is clear that, these cell adhesion studies highly dependent on the sample properties and also the cell type.

4.4.2 MTT assays with NIH3T3 Cell Lines

Fibroblasts are the cells are very important for body since these cells synthesize the extracellular matrix and collagen. There are several studies about the enhancement of fibroblast proliferation [67], that's why, the system used with MG63 cells might be an alternative system for enhancement of proliferation of these cells. For this reason, MTT assays were done with the samples explained in Section 3.4.2 and the effect of incubation time can be seen from Figure 4.19, 4.20 and, 4.21.

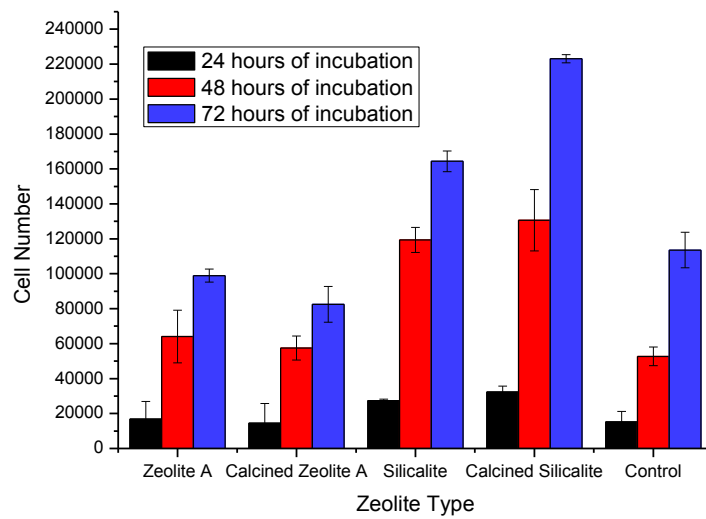


Figure 4.19 MTT assay results for various samples for 24, 48, and 72 hours of incubation for NIH 3T3 Cell Line with 0.125 cm² zeolite coated samples.

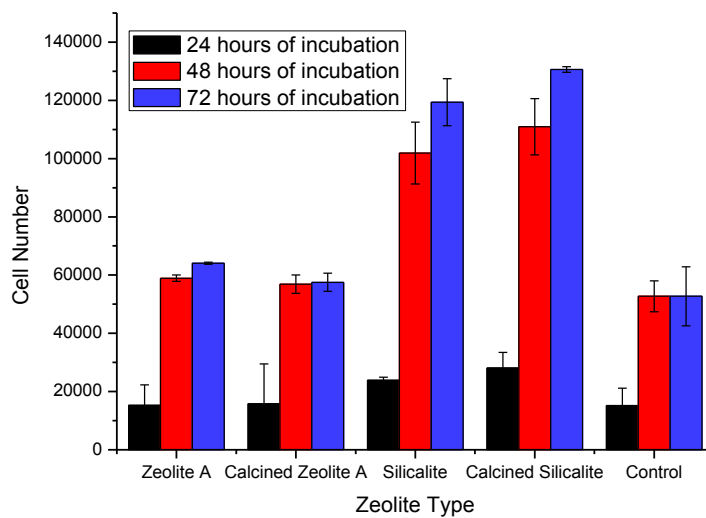


Figure 4.20 MTT assay results for various samples for 24, 48, and 72 hours of incubation for NIH 3T3 Cell Line with 0.08825 cm² zeolite coated samples.

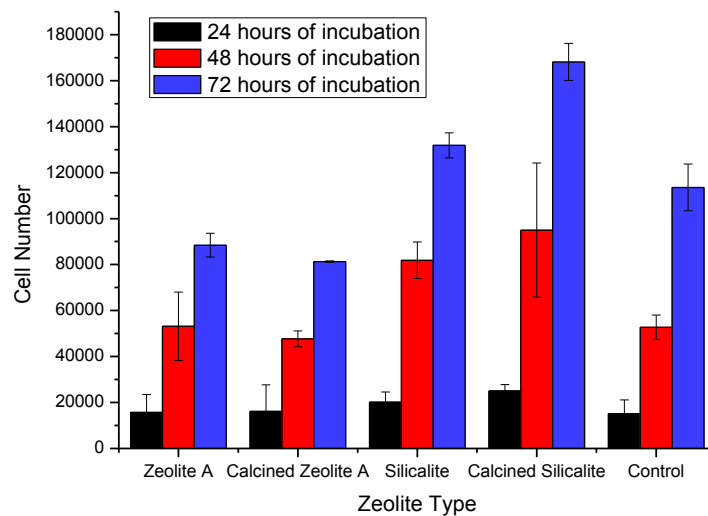


Figure 4.21 MTT assay results for various samples for 24, 48, and 72 hours of incubation for NIH 3T3 Cell Line with 0.04167 cm^2 zeolite coated samples.

Figures 4.19, 4.20, and 4.21 showed that with increasing time, number of cells on samples increase. This has the same correlation with MG63 cell line results. Also in the same manner, silicalites were better than Zeolite A's. There are several differences between silicalites and zeolite A's. Silicalites have larger particle diameters, and more positive surface charges compared to zeolite A's. There are some studies about the effect of the surface charge on cell adhesion, and also our results indicates that more hydrophobic and positively charged samples, which are silicalites have more number of cells on them after 24, 48 and 72 hours with each cell lines. Also particle size of the zeolites are quite different than each other, silicalites are approximately 500 nm in diameter while zeolite A's are 300 nm's.

Figure 4.22, 4.23, and 4.24 shows the effect of zeolite amount on the samples with respect to number of cells after 24, 48 and 72 hours respectively.

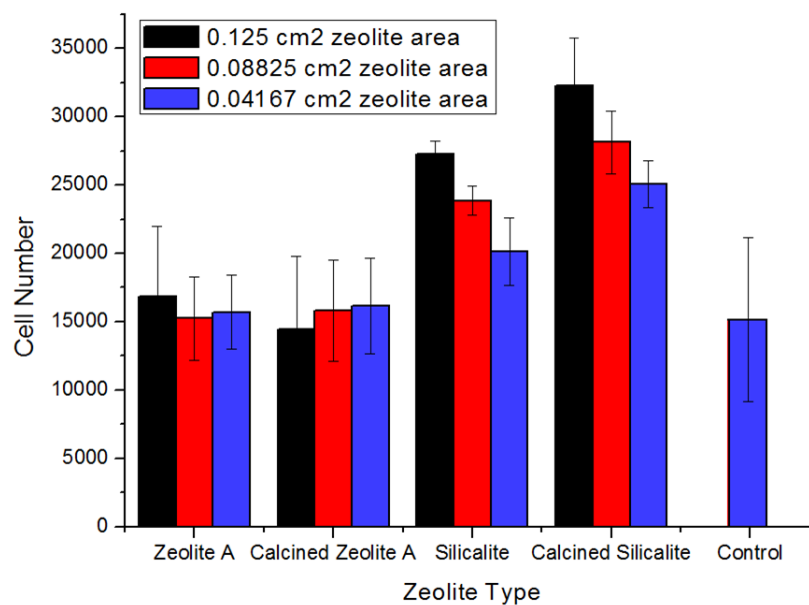


Figure 4.22 MTT assay results for various samples with 0.125, 0.08825, and 0.04167 cm² zeolite patterned area for NIH 3T3 Cell Line for 24 hours incubation.

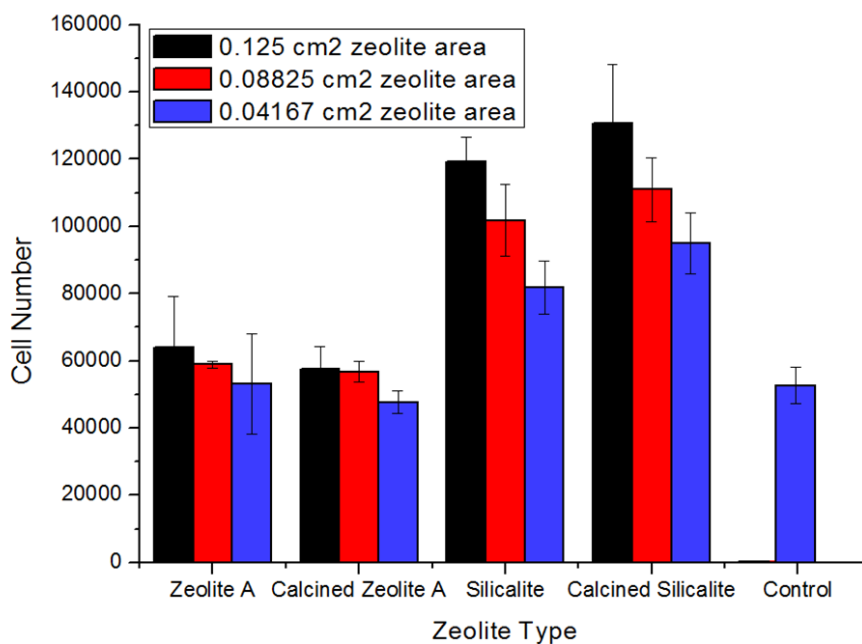


Figure 4.23 MTT assay results for various samples with 0.125, 0.08825, and 0.04167 cm² zeolite patterned area for NIH 3T3 Cell Line for 24 hours incubation.

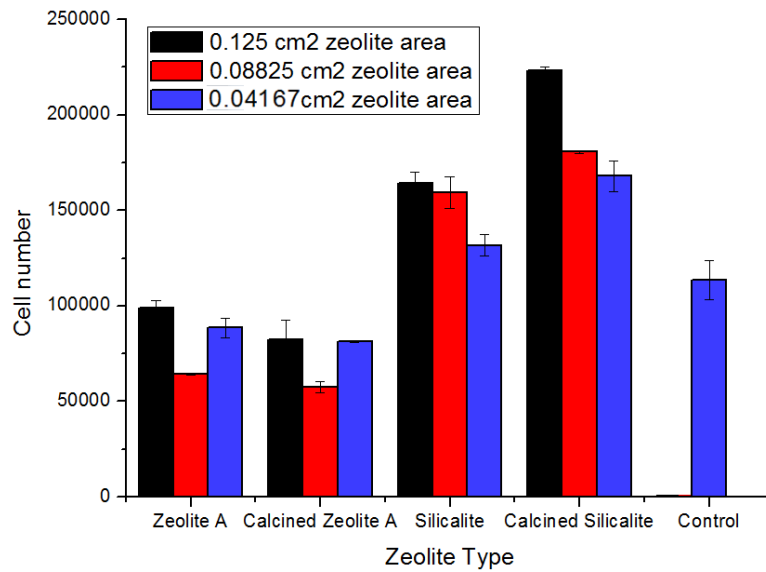


Figure 4.24 MTT assay results for various samples with 0.125, 0.08825, and 0.04167 cm² zeolite patterned area for NIH 3T3 Cell Line for 24 hours incubation.

Similar to the results obtained with MG63 cell line, silicalite and calcined silicalite coated samples showed an increasing trend with increase in the zeolite coated areas. Statistical analysis showed that there is a significant difference between 0.04167cm² silicalite coated samples and 0.125 cm² silicalite coated samples after 48 and 72 hours of incubation (p=0.042 and 0.052 respectively) while there this number of cell difference is significant between 0.04167cm² calcined silicalite coated samples and 0.125 cm² calcined silicalite coated samples after 24, 48 and 72 hours of incubation (p=0.05, 0.038 and 0.028 respectively).

Similar to the results with MG63 cell line, surprisingly calcination makes different effect on two different zeolites. Calcination increases the total cell amount on silicalite samples, while it decreases cell number on zeolite A samples. Fengolio et al. [66] reported that internal surface of the zeolites are does not play a role on

cell adherence since the pores are so small and Petushkova et al. [68] showed that again internal surface areas of silicalite does not play a role while, larger surface areas are more cytotoxic. In this study, there is a significant difference on calcined samples observed, and it can be explained by the adsorption of proteins in the media can be adhered on the pores, at least at the pore openings of the zeolites and it may enhance the adherence and proliferation of the cells on samples.

4.5 Conductometric Biosensor Measurements

Conductometric biosensor electrodes modified with zeolites with the procedure explained in 3.3.1 and several biosensor measurements are done with that electrodes and compared with the unmodified standard membrane transducers.

4.5.1 Response Characteristics of Silicalite Modified Electrodes

Zeolite coated conductometric thin-film electrodes were investigated with urease for urea determination. The response curves as a function of urea concentration is shown in Figure 4.25.

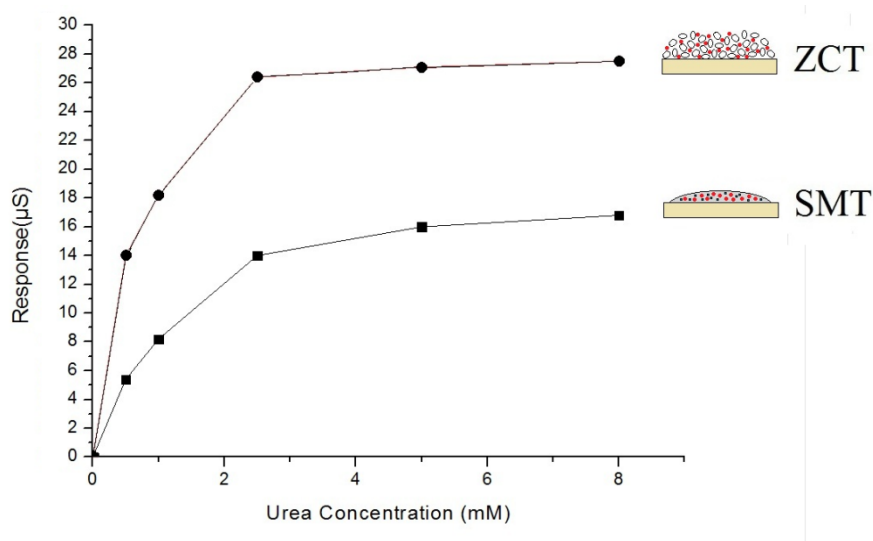


Figure 4.25 Comparison of response curves obtained for ZCTs with SMTs for urea determination for conductometric biosensors.

As shown in Figure 4.25, using silicalite thin film electrodes as a means for modifying the electrode surfaces before getting any biosensor measurements lead to an increased response in comparison with the standard membrane transducers (SMT). This increased response was significantly higher for ZCT (0.275 μS) with respect to SMT (0.168 μS) type electrodes for 8 mM urea injection.

Although, this had been a first time investigation of such an approach for modified electrodes in urease measurements using conductometric biosensors, the effect of adding zeolites into the enzyme containing membranes was studied using different zeolites and electrochemical biosensors. The effect of zeolite addition on enzymatic activity using NaY as the zeolitic material and cutinase as the enzyme was deeply investigated using fluorescence emission spectra by Vidinha et al. [69]. Their results indicated that placing the zeolite in close proximity to the enzyme improved the accessibility of the enzyme to the substrate and lead to higher enzymatic activity. Zhou et al. [40] also made a similar discussion constructing a layer-by-layer ITO electrode surface using zeolite Beta for the

adsorption of enzymes and measuring their amperometric responses. They proposed that zeolite addition enhanced the effective spaces of the surface of modified electrodes for enzyme immobilization. In the current study, the conductometric electrode surfaces were modified by silicalite type zeolites for the first time for urea determination and similar enhancements were observed for ZCT type electrodes.

The response curves of the conductometric biosensor as a function of time upon addition of urea is also shown in Figure 4.26.

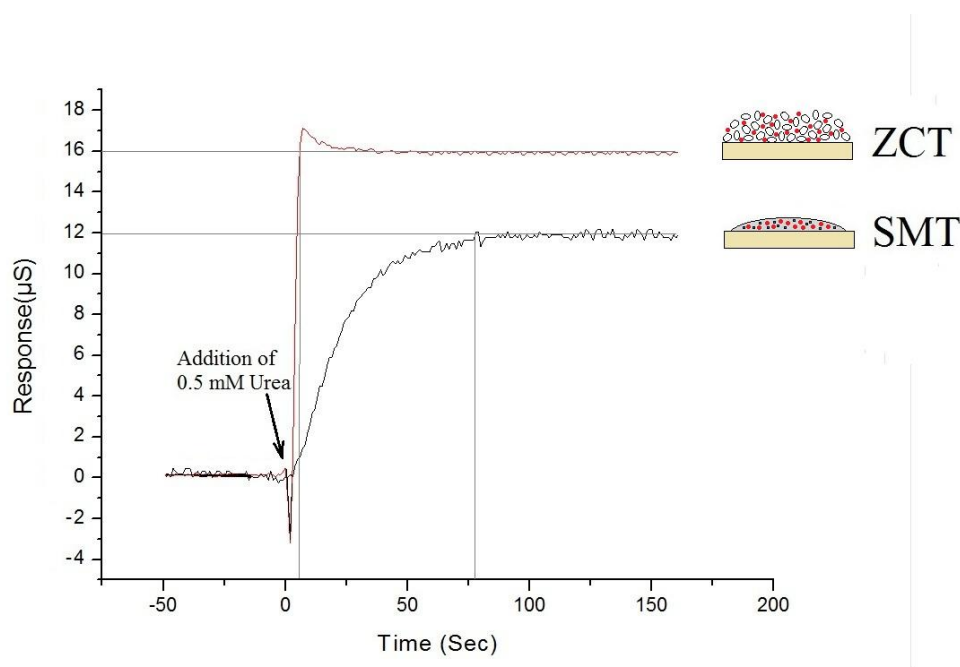


Figure 4.26 Response curves of conductometric biosensor based on urease ZCTs and SMTs.

As shown in Figure 4.26, after the biosensor reached a stable response value in blank phosphate buffer solution, injection of urea stock solution caused significantly faster sensor response in ZCT electrodes. This might be due to GA

layer on top of the transducer in SMTs, which may be considered as a diffusion barrier. Full response was reached for SMT in ca. 80 seconds, while it only took about 8 seconds to reach the full performance for the ZMT biosensors. These results were significantly shorter than the ones obtained by Lee et al. using silica sol-gel matrix in which they obtained steady state values in 16.5 minutes [70]. They claimed that the long response times were due to the relatively thick sol-gel films of 25 ± 2 μm . In the current study, the thicknesses of the films were measured as 5 ± 1 μm . Thus, the applied methodology in this work to modify electrode surfaces also gives the advantage to coat the surfaces in a more controlled manner with respect to the traditional sol-gel methodologies. Even only a single crystal thickness could be attained on various electrode surfaces if desired [56, 71]. It can be hypothesized that the reason for the observed significant decrease in the time spent to reach equilibrium response values after the injection of urea is again due to the enhanced effective spaces of the surface of modified electrodes for enzyme immobilization. This property, in addition to the hypothesized biocompatibility of zeolitic materials can be important for applications, which require fast responding sensors. To have a full understanding of the biosensor related properties of the ZCT type conductometric electrodes, operational and storage stabilities were also investigated.

4.5.2 Operational and Storage Stabilities of Silicalite Modified Electrodes

The practicability of biosensors is often limited by its operational and storage stability. For the ZCT electrodes, the operational and storage stabilities were tested over a 400 minutes and 150 hours periods respectively by monitoring the

responses to the injection of 1 mM of urea. The results of the storage and operational stability experiments are shown in Figure 4.27.

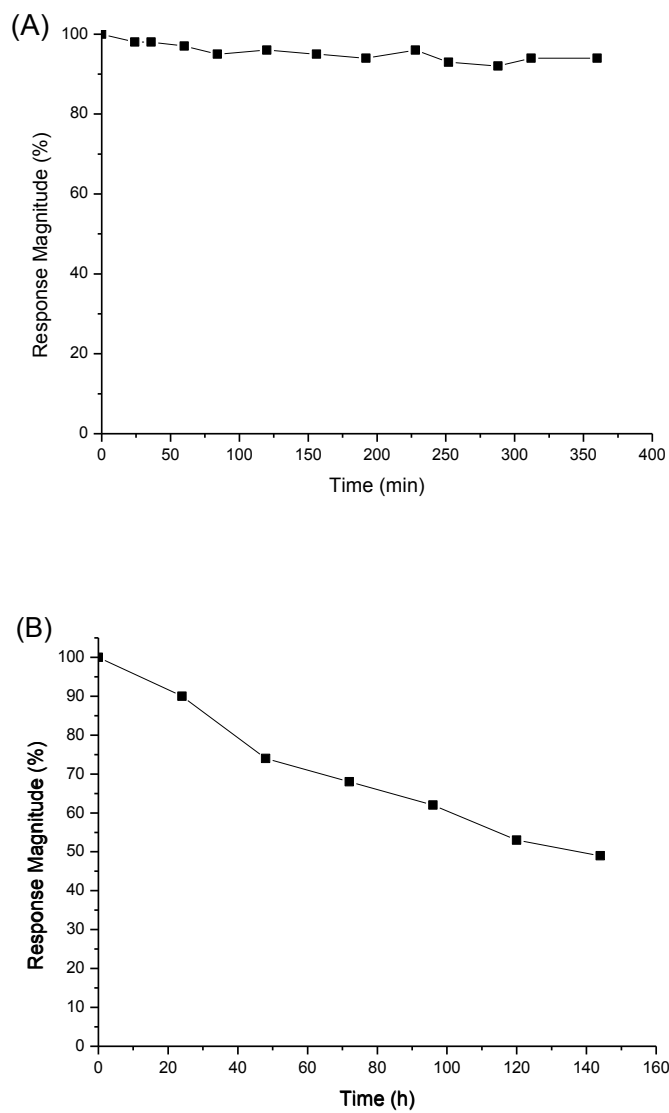


Figure 4.27 Operational (A) and storage (B) stability results of ZCTs with Silicalite.

According to the operational stability results, ZCTs almost retained their original activity for 350 minutes. Furthermore, the prepared ZCT's stored 50% of their original activity after 144 hours, which is acceptable for conductometric biosensors. Lee et al. [72, 73] reported that conductometric sol-gel immobilized urease biosensor used with commercial urea stored 50% of its original activity after 3 weeks and same type biosensors used with serum, stored 63% of its original activity after 3 weeks, which is comparable with ZCT results.

The adsorption of proteins on inorganic substrates can be seen as a simple phenomenon; however there are many different parameters that can be effective in this matter [74]. The interaction of enzymes with zeolites can actually be complicated due to different factors, such as hydrophilic and hydrophobic, electrostatic, and/or structural interactions. Tavolaro et al. [74] showed that protein adsorption on zeolites can be influenced by the Brønsted acidity of the zeolite. It is well known that enhanced catalytic activities can be gained through a controlled variation in the number and strength of framework Al-OH-Si groups (i.e., Si/Al ratio) that are known to be the Brønsted acid sites in zeolites. There are various studies in the literature trying to investigate the interaction between the zeolites and proteins on a systematic basis by changing the acidic properties of zeolites, however these investigations are usually made by changing the zeolite type, and thus the zeolite structure [74]. On the other hand, once the structure is changed hoping to alter the acidity of the zeolite for such an investigation, many different parameters are also changing, like the overall nature and density of the defect sites, the external surface area, surface roughness and morphology, pore sizes, etc.

Accordingly, in the current study, it was aimed to make a more systematic investigation on the effect of Brønsted acidity in terms of whether it really has an influence or not on the obtained activities on the ZCT conductometric biosensors

by using the same type of zeolite, which is zeolite Beta. Zeolite Beta, a wide-pore zeolite, can be ideally used to study a wide range of Si/Al ratio without the necessity to change the zeolite type to obtain varying Brønsted acidities in the same structure [75]. Thus, comparison of conductometric urea biosensor responses obtained using ZCT type electrodes was performed using zeolite Beta with three different Si/Al ratio of 40, 50, and 60 in the current study for the first time.

4.5.3 Effect of Si/Al ratio on Conductometric Urea Biosensors

In this study, a new method as shown in Figure 3.1(C) and denoted as “ZCT” was tested and studied to modify conductometric transducer surfaces using zeolite Beta to investigate the effect of changing Si/Al ratio. The results obtained were compared by the “Standard membrane transducers” (SMT) which contains no zeolite and zeolite membrane transducers (ZMT) where the enzymatic solution contains zeolite Beta nanoparticles as an alternative technique. In general, it was aimed to investigate whether the prepared zeolite film on the transducers were going to maintain surface characteristics of zeolite Beta nanoparticles by observing whether different and especially consistent responses were going to be obtained as a function of changing Si/Al ratio. In this method, surfaces of the transducers were directly coated with zeolite Beta nanoparticles with Si/Al ratio of 40, 50, and 60. Then 0.1 μ l, 5% urease solution in phosphate buffer solution was dropped by a micropipette onto the working electrode side and 0.1 μ l, 5% BSA in PBS was dropped onto the reference electrode side of the electrode. By doing so, GA was avoided, which is known to inactivate the enzymatic activity of membrane [62].

For this purpose, firstly “zeolite modified transducers” (ZMT) were tested against the “standard membrane transducers” (SMT) for zeolite Beta with varying Si/Al ratio (BEA40, BEA50, and BEA60) mixed enzymatic membranes on the conductometric biosensors. The comparison of calibration curves obtained among ZMT’s with BEA40, BEA50 and BEA60 and SMT’s are shown in Figure 4.28.

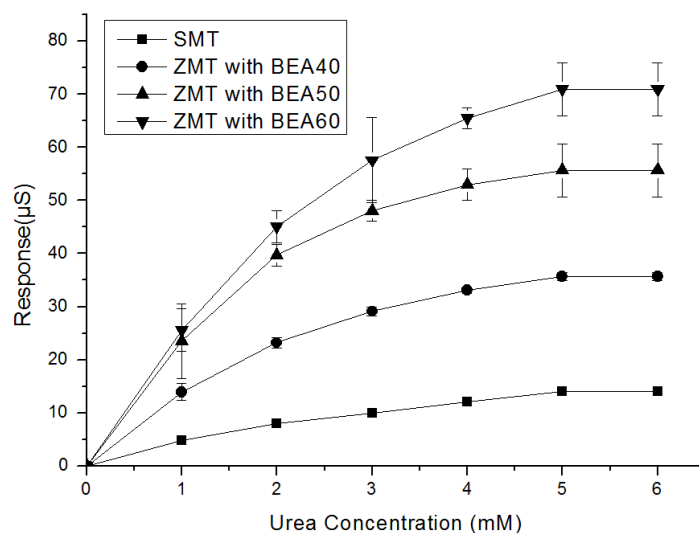


Figure 4.28 Comparison of responses obtained using ZMTs prepared using BEA40, BEA50 and BEA60 and SMT type conductometric biosensors.

The Si/Al ratio of zeolites is used to denote the hydrophobicity of zeolites, with higher ratios indicating a higher degree of hydrophobicity and lower ion-exchange capacity. The morphology of the zeolite structure varies [69].

In this process, interactions between the support and the guest molecules are of non-covalent nature, such as hydrogen bonding, electrostatic, van der Waals and hydrophobic or hydrophilic interactions, thus relatively weak. The immobilization techniques, however, could affect their catalytic activity.

Figure 4.28 shows the conductometric enzymatic responses of all ZMT and SMT electrodes obtained after the addition of urea solution into 5 mM phosphate buffer solution. According to Figure 4.28, all ZMT's showed higher responses with respect to the traditional SMT's. It is known that for large zeolite particles, the outer surface of zeolite crystals possesses about 5-10% of the total zeolite surface. Even for such cases, there will still be a relatively large surface interaction between zeolite and biological species due to the highly dispersed zeolites in the membrane [76]. Accordingly, it can be seen that there had been an increased interaction between the zeolite nanoparticles and the enzyme leading to an increased response obtained using all ZMT's.

Furthermore, it can be seen that the conductometric responses increased with increasing Si/Al ratio for ZMT type electrodes. As shown in Figure 4.28, the highest response was obtained from BEA60 and the lowest from BEA40, with the medium response obtained from BEA50. This correlation also indicates that there had really been some sort of interaction between the zeolite nanoparticle surface and the enzyme for each particular case. This behavior can be due to an increased hydrophobicity and/or the increasing acidic strength with the increasing Si/Al ratio within the zeolite crystals. Mintova et al. [77] clearly discussed the results showing that high Al containing HZSM-5 possessed more hydrophilic active sites, while the zeolites with low Al content showed the opposite characteristics. Accordingly, the changing Brønsted acidity and the hydrophilicity of zeolites are interrelated and cannot be discussed as separate factors affecting the protein adsorption on zeolites. The studies showed that acid strength increase with the decrease of the aluminum atoms in the zeolite [62, 78]. Furthermore, in the literature it was seen that number and the mobility of the zeolitic cations play an essential role in charge transfer across the membrane phase and do significantly influence the responses [79]. Accordingly, the results obtained and shown in Figure 4.28 clearly demonstrate the changing biosensor response as a function of

acidity and the hydrophilicity of zeolite Beta for conductometric urea biosensor for the first time.

The effect of directly modifying the electrode surface with different types of BEA type zeolites was also investigated to study whether a similar response correlation was going to be obtained as a function of Si/Al ratio and if the ZCT and ZMT responses were going to be different than each other for each type of zeolite. Accordingly, the conductometric responses obtained using BEA50 and BEA60 is shown for ZMT and ZCT type electrodes in comparison with the responses obtained on the SMT and the results are shown in Figure 4.29.

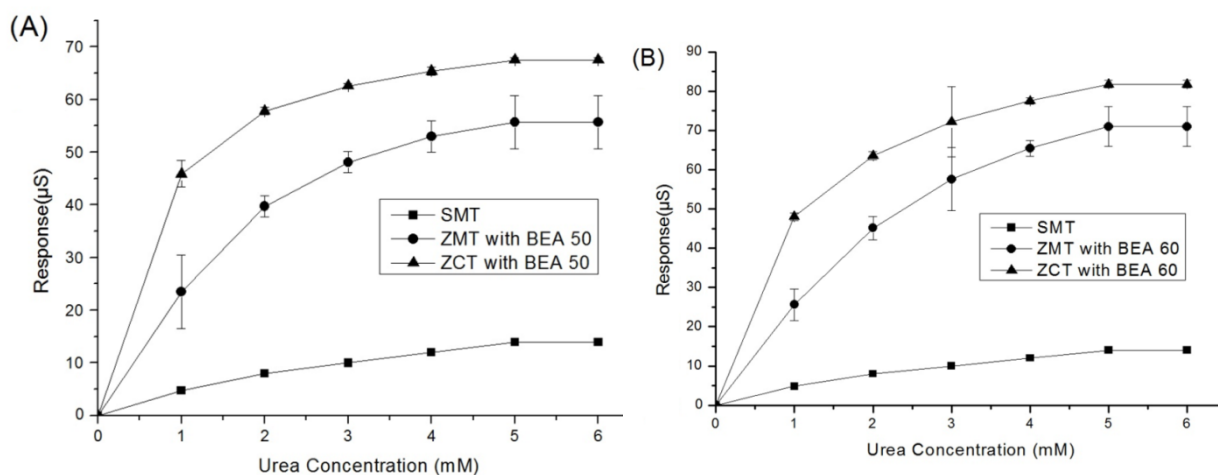


Figure 4.29 Comparison of the calibration curves between SMT, ZMT, and ZCTs using zeolite BEA50 (A) and BEA60 (B).

As shown in Figure 4.29, Zeolite Coated Transducers (ZCTs) gave higher responses from both SMTs and ZMTs. The membranes in SMT and ZMT technique has very low reproducibility due to cast a very thin film on transducer surface and it is almost impossible to cast the same film in every trial. When

compared with SMTs and ZMTs, ZCTs have higher reproducibility due to the controlled thickness of zeolite thin film by dip coating, and the known amount of enzyme adsorbed to this film. Moreover, glutaraldehyde which can be considered as a diffusion barrier and a poisonous chemical for enzymes is not used in ZCTs.

4.5.4 Effect of Zeolite Modification with Silver and MV on Conductometric Urea Biosensors

To understand the effect of the silver and methylviologen modification on zeolites, the zeolite membrane transducers (ZMT) prepared with Ag^+ , Ag^0 and MV modified electrodes compared with standard membrane transducers (SMT) and unmodified zeolite membrane transducers.

Table 4.4 Effect of zeolite modification on Conductometric Biosensor Transducers.

	Relative Biosensor Responses			
	w/o zeolite	Zeolite Beta 40	Zeolite Beta 50	Zeolite Beta 60
Standard Membrane Transducer	29.3	-	-	-
Zeolite Membrane Transducer	-	75.6	78.1	100
MV-Zeolite Membrane Transducer	-	70.7	58.5	97.6
Ag ⁺ -Zeolite Membrane Transducer	-	0	0	0
Ag ⁰ -Zeolite Membrane Transducer	-	0	0	0

The responses are normalized to 100 which is Zeolite coated transducers with zeolite Beta 60. Methylviologen modification has no significant effect on conductometric biosensor responses while silver in both ion and nanoparticle forms didn't give any responses in conductometric biosensor measurements.

CHAPTER 5

CONCLUSIONS

In this study, various zeolites were attached onto conductometric biosensor transducers and also were patterned on silicon wafers with electron beam lithography and photolithography approaches. Aside from the biosensor studies, in order to investigate the possibility of using zeolites in biomedical applications, the effect of silicalite and zeolite A on cell viability studies were also investigated. For the biosensor studies, zeolite Beta crystals with Si/Al ratios of 40, 50, and 60 were synthesized. The cell related studies were conducted using the synthesized zeolite A and silicalite nanocrystals.

The first part of this study was to investigate the ability of patterning zeolite A and silicalite particles on silicon wafers. The combination of direct attachment method and e-beam lithography lead to full control on patterns with both width, height in nanometer level of resolution, and coverage of the zeolite coated areas. For this purpose, various different lithographic patterns were successfully fabricated using silicalite and zeolite A. In that way, it was possible to obtain nano-sized patterns, i.e., 200-500 nm, in full control. In order to obtain larger sized patterns with more zeolite coverage, photolithographic technique was also applied similarly. In this case, minimum feature size was 5 μm and the patterned area was in centimeter scale. This combination of direct attachment and lithographic approach resulted in the fabrication of zeolite patterns ranging from 500 nm to 100 μm feature size for the first time.

Another study was conducted to fabricate two different types of zeolites, silicalite and zeolite A, with varying surface properties on the same silicon substrate with a control of zeolite pattern sizes ranging from 500 nm to 100 μm by direct attachment methodology. This method allowed one to have a better control on differentiated areas on surfaces. For this purpose, various patterns were fabricated, where silicalite line patterns were formed on zeolite A monolayer and vice versa with the help of electron beam lithography and photolithography. Furthermore, thickness of the features created on zeolite monolayer film was controlled by the resist thickness of both electron beam lithography and photolithography systems.

The second part of this study was to investigate the effect of different zeolite modification techniques on conductometric urea biosensors. For that purpose two different modifications were applied, which were zeolite coated transducers (ZCT) and zeolite membrane transducers (ZMT), and these transducers were compared with standard urea membrane transducers (SMT).

Firstly, the effect of zeolite coating on the response characteristics and stability of conductometric transducers were investigated with silicalite crystals. The zeolite coated transducers (ZCT) showed approximately 100% higher signals than the standard membrane transducers (SMT) within 8 seconds of maximum response reaching time for 0.5 mM urea addition, which was approximately 80 seconds for SMTs. The acquired enhancement upon using ZCTs can be related with the obtained relatively thin zeolite films on the transducer surfaces, which lead to fast transfer of ions that are close to the transducer surface and the lack of GA layer. Since the stability of the transducers in both operation and storage conditions are the most important parameters for biosensors, these parameters of ZCTs were also investigated. Results showed that ZCTs kept their original activities after 6 hours of operation and 50% of their original activity after 144 hours of storage in +4 $^{\circ}\text{C}$, dry conditions.

Two different modifications, ZMT and ZCT, of conductometric biosensor transducers were compared with SMT to better understand the zeolite enzyme interactions using zeolite Beta crystals which have Si/Al ratios of 40, 50, and 60. It was found that zeolite addition into membranes (ZMT) enhanced biosensor signal using all zeolite types when compared with SMT, while signals obtained from ZCTs were significantly higher than both SMT and ZMT. The enhancement observed upon using ZMTs can be due to the zeolitic cations, which have ability to transfer charge from media to the transducer. Additionally, the maximum enhancement observed upon using ZCTs can be due to the lack of GA layer that exists on top of the film in both SMTs and ZMTs, which results in the inhibition of enzymes. Also membranes obtained using SMTs and ZMTs technique had very low reproducibility, which can be due to the casting problem that is done by exposing the transducer to GA vapor. Furthermore, transducers fabricated using ZCT method showed higher reproducibility when compared with SMTs and ZMTs, due to the controllable thickness of the zeolite film that was done by dip coating.

The Si/Al of the zeolites can be used to represent the acidity of the zeolites and this acidity can be controlled with the number and strength of the framework Al-OH-Si groups, which are known as Brønsted acid sites. Thus, zeolite Beta crystals with Si/Al ratio of 40, 50, and 60 were used to build ZMTs and the results obtained were compared with data gathered using SMT. It was observed that the increase in the Si/Al ratio resulted in an enhancement of biosensor signals. It may be due to the better interaction formed between the enzyme and zeolite as a result of increased hydrophobicity and acid strength with increasing Si/Al ratios. This new approach can be applicable to all kinds of electrochemical biosensors since it is easy to produce these transducers and they have good storage and working stabilities with enhanced signals.

In the third part of the study, it was aimed to use the obtained zeolite patterned substrates in an actual biomedical application to see whether any changes were going to be attained at all as a function of calcination and changing zeolite amount and zeolite type for the first time. For this purpose, an array of line varying in size composed of zeolites was patterned on silicon substrate to study the effect of the zeolite patterns on cellular behavior. Zeolite A and silicalite were patterned on 1 cm² wafer pieces by photolithography technique with zeolite patterned areas of 0.125, 0.08825, and 0.04167 cm². Viability of MG63 osteoblasts and NIH3T3 fibroblasts was assessed through the MTT assays after 24, 48, and 72 hours of incubation with an initial cell concentration of 2×10^4 cells/sample of zeolite A and silicalite patterned surfaces. In addition, the calcined and as-synthesized zeolite A and silicalite nanoparticles were patterned in the same manner in order not only to investigate the effect of zeolite type, but also the effect of zeolite amount and calcination of zeolites on cell proliferation.

Results showed that the cell proliferation was higher on zeolites with respect to the control group. Silicate patterned samples showed however the highest proliferation rate among all samples. This could be associated with the presence of positive charges on the surface and hydrophobic nature of the silicalite nanoparticles in comparison to zeolite A nanoparticles.

Interestingly, calcination increased the total number of both osteoblasts and fibroblasts. As known, calcination increases the internal surface area by opening pores. Therefore, our results suggest that pores play a significant role in the cell proliferation. As such, changing different zeolitic surfaces would lead to different cell behavior, and cell proliferation can readily be modulated by changing the amount and type of zeolites.

REFERENCES

- [1] M. E. Davis, R. F. Lobo, *Chem. Mater.* 4 (1992) 756.
- [2] E. Soy, Immobilization of Proteins on Zeolite and Zeo-Type Materials for Biosensor Applications Based on Conductometric Biosensors and Ion Sensitive Field Effect Transistors. MS thesis, 2011.
- [3] Ş.B. Tantekin-Ersolmaz, Ç. Atalay-Oral, M. Tatlıer, A. Erdem-Şenatalar, B. Schoeman, J. Sterte, *J. Membr. Sci.* 175 (200) 285.
- [4] S. Mintova, V. Valtchev, T. Onfroy, C. Marichal, H. Knözinger, T. Bein, *Microp. Mesop. Mater.* 90 (2006) 237.
- [5] E. Soy, V. Pyeshkova, V. Arkhypova, B. Khadro, N. Jaffrezic-Renault, A. Sacco Jr., S. V. Dzyadevych, B. Akata Kurç, *Sens. Electr. and Micros. Techn.* 1 (2010) 28.
- [6] J. Sárkány, *Appl. Catal. A*, 188 (1999) 369 .
- [7] A. Tavolaro, P. Tavolaro, and E. Drioli, *Colloids Surf. B: Biointerfaces* 55 (2007) 67.
- [8] R. S. Bedi, L. P. Zanello, Y. Yan, *Adv. Funct. Mater.* 19 (2009) 3856 .
- [9] T. T. Andrew, *Nature*, 412 (2001) 491.
- [10] T. J. W. G. Balasundaram, *J. Mater. Chem.* 16 (2006) 3737.
- [11] C. E. Firling, G. L. Evans, G. K. Wakley, J. Sibonga, *J. Bone Miner. Res.* 11 (2009) 254.

- [12] C. Yang, , L. Huang, T. Shen, J. A. Yeh, *Eur. Cell Mater.* 20 (2010) 415.
- [13] T. Ceyhan, M. Tatlier, H. Akçakaya, *J Mater Sci: Mater Med* 18 (2007) 1557.
- [14] M. Gerard, A. Chaubey, B.D. Malhotra, *Biosens. Bioelect.* 17 (2002) 345 .
- [15] D. R. Thévenot, Klara Toth, R. A. Durst, G. S. Wilson, *Biosens. Bioelect.* 16 (2001) 121.
- [16] C. Shan, H. Yang, J. Song, D. Han, A. Ivaska and L. Niu, *Anal. Chem.* 81 (2009) 2378.
- [17] B. Liu, R. Hu, J. Deng, *Anal. Chem.* 69 (1997) 2343.
- [18] O.Y. Saiapina, V.M. Pyeshkova, O.O. Soldatkin, V.G. Melnik, B. Akata Kurç, A. Walcarius, S.V. Dzyadevych, N. Jaffrezic-Renault, *Mater. Sci. Eng. C* 31 (2011) 1490.
- [19] E. Soy, V. Arkhypova, O. Soldatkin, M. Shelyakina, S. Dzyadevych, J. Warzywoda, A. Sacco Jr., B. Akata, *Mater. Sci. Eng. C* (2012) in press.
- [20] T. Yu, Y. Zhang, C. You, J. Zhuang, B. Wang, B. Liu, Y. Kang, Y. Tang, *Chem. Eur. J.* 12 (2006) 1137.
- [21] M. Arvand, S. Sohrabnezhad, M.F. Mousavi, M. Shamsipur, M.A. Zanjanchi, *Anal. Chim. Acta* 491 (2003) 193.
- [22] A. Pallandre, K. Glinel, A.M. Jonas, B. Nysten, *Nano Lett.* 4 (2004) 2.
- [23] G.-J. Zhang, T. Tanii, T. Zako, T. Funatsu, I. Ohdomari, *Sens. Actuators B, Chem.* 97 (2004) 243.
- [24] P.E. Lobert, D. Bourgeois, R. Pampin, A. Akheyar, L.M. Hagelsieb, D. Flandre, J. Remacle, *Sens. Actuators B, Chem.* 92 (2003) 90.

- [25] T. Tanii, T. Hosaka, T. Miyake, G.-J. Zhang, T. Zako, T. Funatsu, I. Ohdomari, *Appl. Surf. Sci.* 232 (2004) 102.
- [26] H.-C. Kim, G. Wallraff, C.R. Kreller, S. Angelos, V.Y. Lee, W. Volksen, R.D. Miller, *Nano Lett.* 4 (2004) 7.
- [27] Z.-H. Wang, G. Jin, *Colloids Surf., B* 34 (2004) 173.
- [28] Y. Huang, W. Shan, B. Liu, Y. Liu, Y. Zhang, Y. Zhao, H. Lu, Y. Tanga, P. Yang, *Lab Chip* 6 (2006) 534.
- [29] Y. Zhang, Y. Liu, J. Kong, P. Yang, Y. Tang, B. Liu, *Small* 2 (2006) 1170.
- [30] Y. Zhang, X. Wang, W. Shan, B. Wu, H. Fan, X. Yu, Y. Tang, P. Yang, *Angew. Chem. Int. Ed.* 44 (2005) 615.
- [31] K. Mukhopadhyay, S. Phadtare, V.P. Vinod, A. Kumar, M. Rao, R.V. Chaudhari, M. Sastry, *Langmuir* 19 (2003) 3858.
- [32] P. Horcajada, A. Rámila, K. Boulahya, J. González-Calbet, M. Vallet-Regí, *Solid State Sci.* 6 (2004) 1295.
- [33] B.G. Trewyn, S. Giri, I.I. Slowing, V.S.-Y. Lin, *Chem. Commun.* (2007) 3236.
- [34] B. Akata, B. Yilmaz, S.S. Jirapongphan, J. Warzywoda, A. Sacco Jr., *Micropor. Mesopor. Mater.* 71 (2004) 1.
- [35] B. Akata, J. Warzywoda, A. Sacco Jr., *J. Catal.* 222 (2004) 397.
- [36] K.B. Yoon, *Acc. Chem. Res.* 40 (2007) 29.
- [37] F. Cucinotta, Z. Popovic, E.A. Weiss, G.M. Whitesides, L.D. Cola, *Adv. Mater.* 20 (2008) 1.

- [38] B. Zhang, M. Zhou, X. Liu, *Adv. Mater.* 20 (2008) 2183.
- [39] C. Leiggener, G. Calzaferri, *ChemPhysChem* 5 (2004) 1593.
- [40] X. Zhou, T. Yu, Y. Zhang, J. Kong, Y. Tang, J-L. Marty, B. Liu, *Electrochem. Commun.* 9 (2007) 1525.
- [41] Z. Popovic, M. Otter, G. Calzaferri, L.D. Cola, *Angew. Chem. Int. Ed.* 46 (2007) 6188.
- [42] K. Ha, J.S. Park, K.S. Oh, Y.-S. Zhou, Y.S. Chun, Y.-J. Lee, K.B. Yoon, *Micropor. Mesopor. Mater.* 72 (2004) 91.
- [43] M.N. Ismail, T.L. Goodrich, Z. Ji, K.S. Ziemer, J. Warzywoda, A. Sacco Jr., *Micropor. Mesopor. Mater.* 118 (2009) 245.
- [44] K. Ha, Y-J. Lee, H.J. Lee, K.B. Yoon, *Adv. Mater.* 12 (2000) 1114.
- [45] G.S. Lee, Y-J. Lee, K. Ha, K.B. Yoon, *Adv. Mater.* 13 (2001) 1491.
- [46] A. Kulak, Y-J. Lee, Y.S. Park, K.B. Yoon, *Angew. Chem. Int. Ed.* 39 (2000) 950.
- [47] J.S. Lee, K. Ha, J.-Y. Lee, K.B. Yoon, *Adv. Mater.* 17 (2005) 7.
- [48] J.S. Lee, J.H. Kim, Y.J. Lee, N.C. Jeong, K.B. Yoon, *Angew. Chem. Int. Ed.* 46 (2007) 3087.
- [49] M. Zhou, X. Liu, B. Zhang, H. Zhu, *Langmuir* 24 (2008) 11942.
- [50] T. Wakihara, S. Yamakita, K. Iezumi, T. Okubo, *J. Am. Chem. Soc.* 125 (2003) 12388.

- [51] S. Galioğlu, M. N. Ismail, J. Warzywoda, A. Sacco Jr., B. Akata, *Micropor. Mesopor. Mater.* 131 (2010) 401.
- [52] J. Choi, S. Ghosh, L. King, M. Tsapatsis, *Adsorption* 12 (2006) 339.
- [53] Z. Wang, Y. Yan, *Micropor. Mesopor. Mater.* 48 (2001) 229.
- [54] G.S. Lee, Y.-J. Lee, K. B. Yoon, *J. Am. Chem. Soc.* 123 (2001) 9769.
- [55] T. C. T. Pham, H. S. Kim, K. B. Yoon, *Science* 334 (2011) 1533.
- [56] S. Öztürk, B. Akata, *Micropor. Mesopor. Mater.* 126 (2009) 228.
- [57] J. Aizenberg, *Adv. Mater.* 16 (2004) 1295.
- [58] W. Sun, K.F. Lam, L.W. Wong, K.L. Yeung, *Chem. Commun.* (2005) 4911.
- [59] S. Li, C. Demmelmaier, M. Itkis, Z. Liu, R. C. Haddon, Y. Yan, *Chem. Mater.* 15 (2003) 2687.
- [60] K. Ha, Y. Lee, D. Jung, J. H. Lee, K. B. Yoon, *Adv. Mater.* 12 (2000) 1614.
- [61] I. Pellejero, M. Urbiztondo, M. Villarroya, J. Sese', M.P. Pina, J. Santamaria, *Micropor. Mesopor. Mater.* 114 (2008) 110.
- [62] R.H. Carvalho, F. Lemos, J.M.S. Cabral, F. Ramôa Ribeiro, *J. Molecular Catal B.* 44 (2007) 39.
- [63] N. Schütze, M.J. Oursler, J. Nolan, B.L. Riggs, T.C. Spelsberg, *J. Cell. Biochem.* 58 (1995) 39.
- [64] P. E. Keeting, M. J. Oursler, K. E. Wiegand, S. K. Bonde, T. C. Spelsberg, B. L., *J Bone Miner. Res.* 7 (1992) 1281.

- [65] E. S. Thian, Z. Ahmad, J. Huang, M. J. Edirisinghe, S. N. Jayasinghe, D. C. Ireland, R. A. Brooks, N. Rushton, W. Bonfield, S. M. Best, *Acta Biomaterialia* 6 (2010) 750.
- [66] I. Fenoglio, A. Croce, F. Di Renzo, R. Tiozzo, B. Fubini, *Chem. Res. Toxicol.* 13 (2000) 489.
- [67] M. A. Mariggio, A. Cassano, A. Vinella, A. Vincenti, R. Fumarulo, L. Lo Muizo, A. Maiorano, D. Ribatti, G. Favia, *Int. J. Immunopathol. Pharmacol.* 22 (2009) 485.
- [68] A. Petrushkov, J. Intra, J. B. Graham, S.C. Larsen, A. K. Salem, *Chem. Res. Toxicol.* 22 (2009) 1359.
- [69] P. Vidinha, V. Augusto, J. Nunes, C. J. Lima, J. Cabra, S. Barreiros, *J. of Biotech* 135 (2008) 181.
- [70] J. Wang, *Electroanalysis* 17 (2005) 7.
- [71] K. Ha, Y. J. Lee, D. Y. Jung, J. H. Lee, K. B. Yoon, *Adv. Mater.* 12 (2000) 1614.
- [72] W. Y. Lee, K. S. Lee, T. H. Kim, M. C. Shin, J. K. Park, *Electroanalysis* 12 (2000) 78.
- [73] W. Lee, S. Kim, T. Kim, K. S. Lee, M. Shin, J. Park, *Anal. Chim. Acta* 404 (2000) 195.
- [74] P. Tավոlаrо, A. Tավոlаrо, G. Martino, *Colloids and Surfaces B* 70 (2009) 98.
- [75] E. A. Aksoy, B. Akata, N. Bac, N. Hasirci, *J. Appl. Poly. Sci.* 104 (2007) 3378.

- [76] P. Tavoraro, A. Tavoraro, Proceedings of the 3rd Congress of Nanotechnology 2006.
- [77] E.P. Ng, S. Mintova, *Microp. Mesop. Mater.* 114, (2008) 1.
- [78] R. G. Leliveld, T. G. Ros, A. J. van Dillen, J. W. Geus, and D. C. Koningsberger, *J. Catal.* 185 (1999) 513.
- [79] S. Matysik, F.M. Matysik, K. D. Schulze, W. D. Einicke, *Electrochimica Acta* 48 (2002) 297.
- [80] L. C. J. Thomassen, A. Aerts, V. Rabolli, D. Lison, L. Gonzalez, M. Kirch-Volders, D. Napierska, P. H. Hoet, C. E. A. Kirschhock, J. A. Martens, *Langmuir* 26 (2010) 328.
- [81] V. Rabolli, L. C. J. Thomassen, F. Uwambayinema, J. A. Martens, *Toxicol. Lett.* 206 (2011) 197.
- [82] T. Ceylan, M. Tatlier, H. Akçakaya, *J. Mater. Sci: Mater. Med.* 18 (2007) 1557.
- [83] B. G. Keselowsky, D. M. Collard, A. J. Garcia, *Biomaterials* 25 (2004) 5947.

APPENDIX A

Literature XRD Diffractograms

1. Zeolite A (LTA)

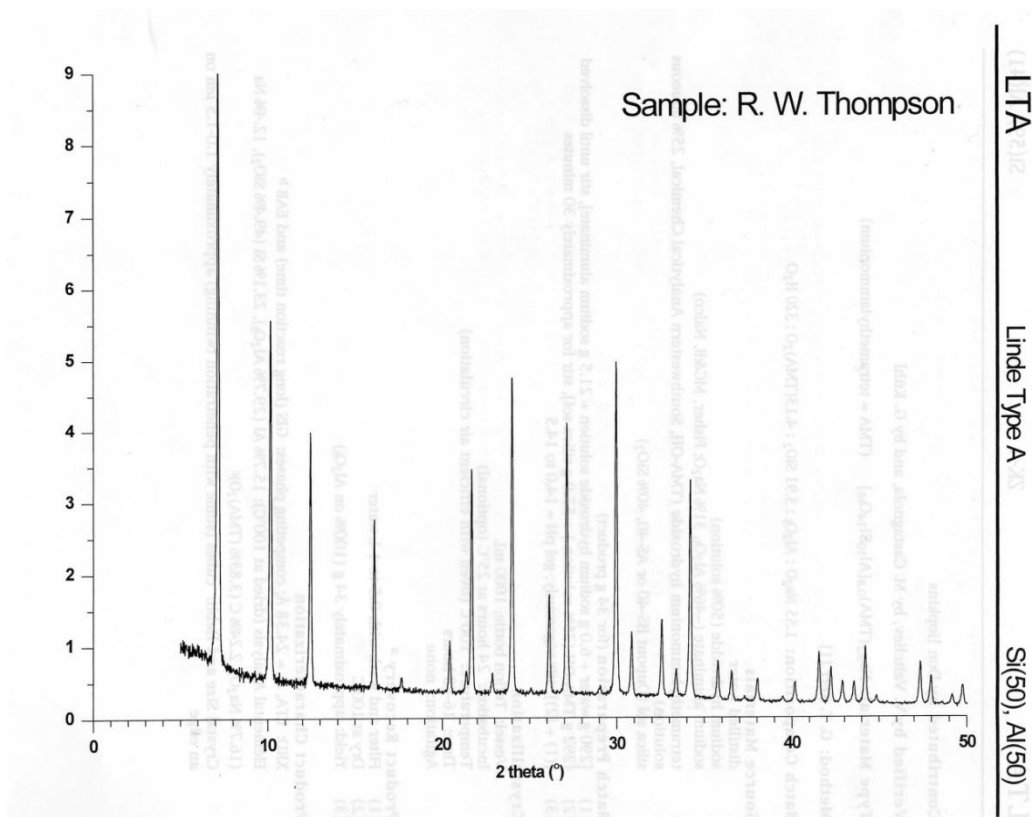


Figure A.1 Literature XRD diffractograms of Zeolite A

2. Zeolite Beta

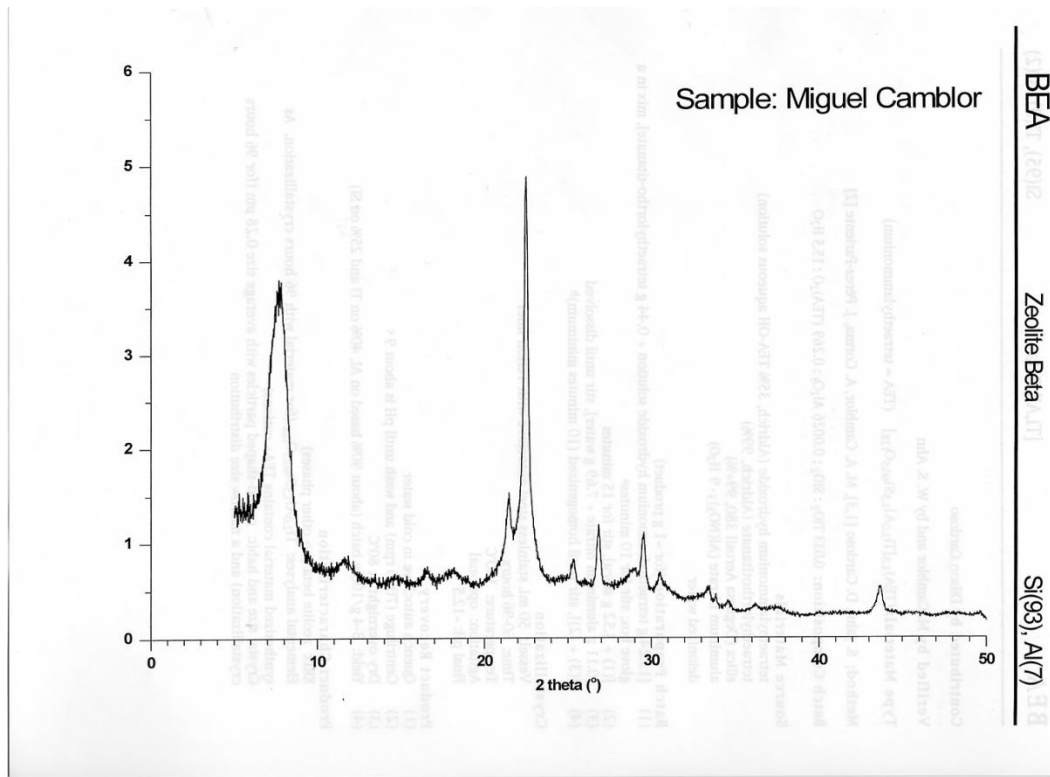


Figure A.2 Literature XRD diffractograms of Zeolite Beta

3. Silicalite

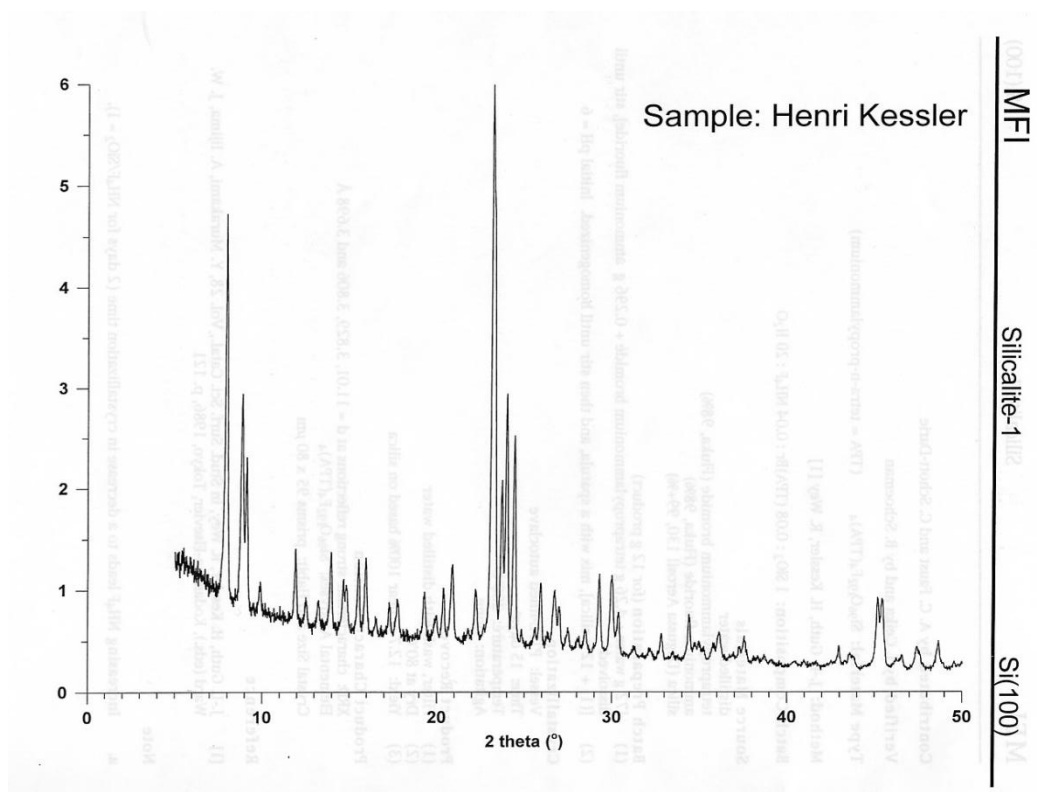


Figure A.3 Literature XRD diffractograms of Silicalite

* Taken from <http://www.iza-online.org>

APPENDIX B

Representative scanning electron microscopy images of prepared various zeolite patterns.

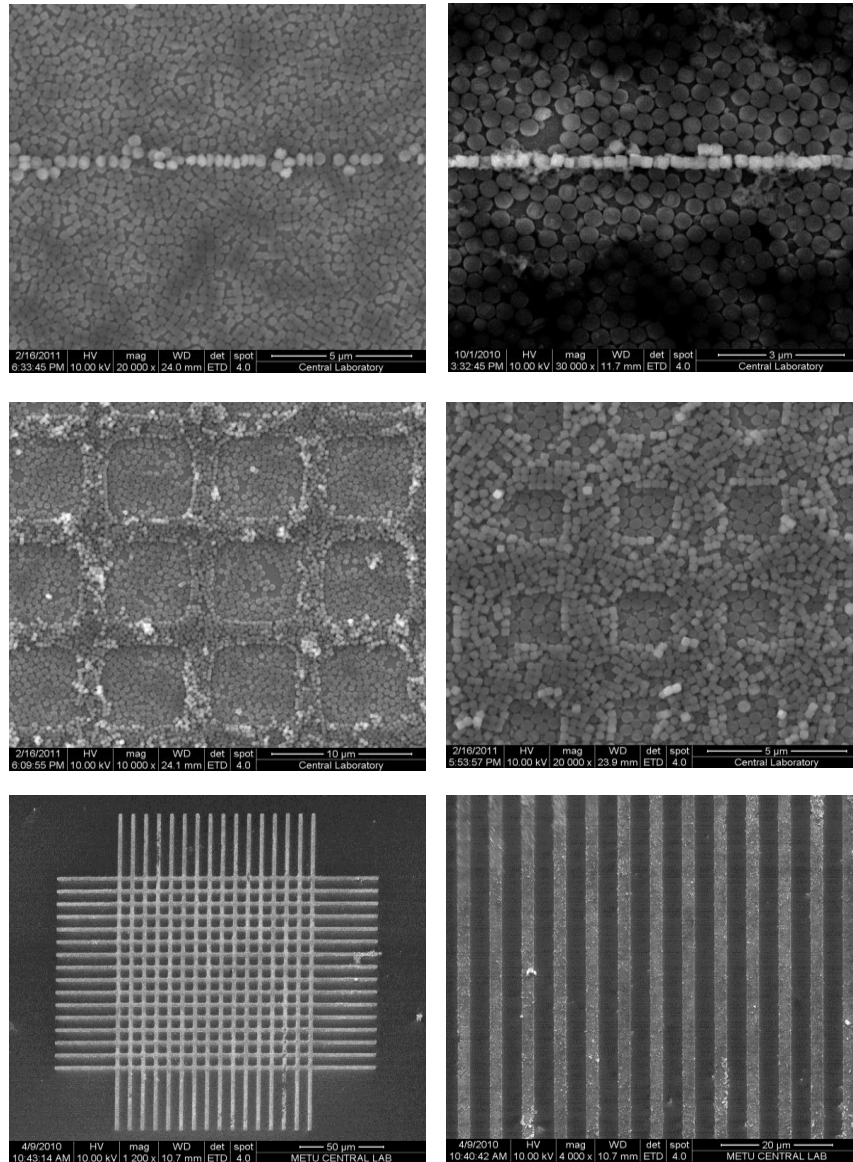


Figure B.1 Representative scanning electron microscopy images of prepared various zeolite patterns

Representative scanning electron microscopy images of prepared various zeolite patterns.

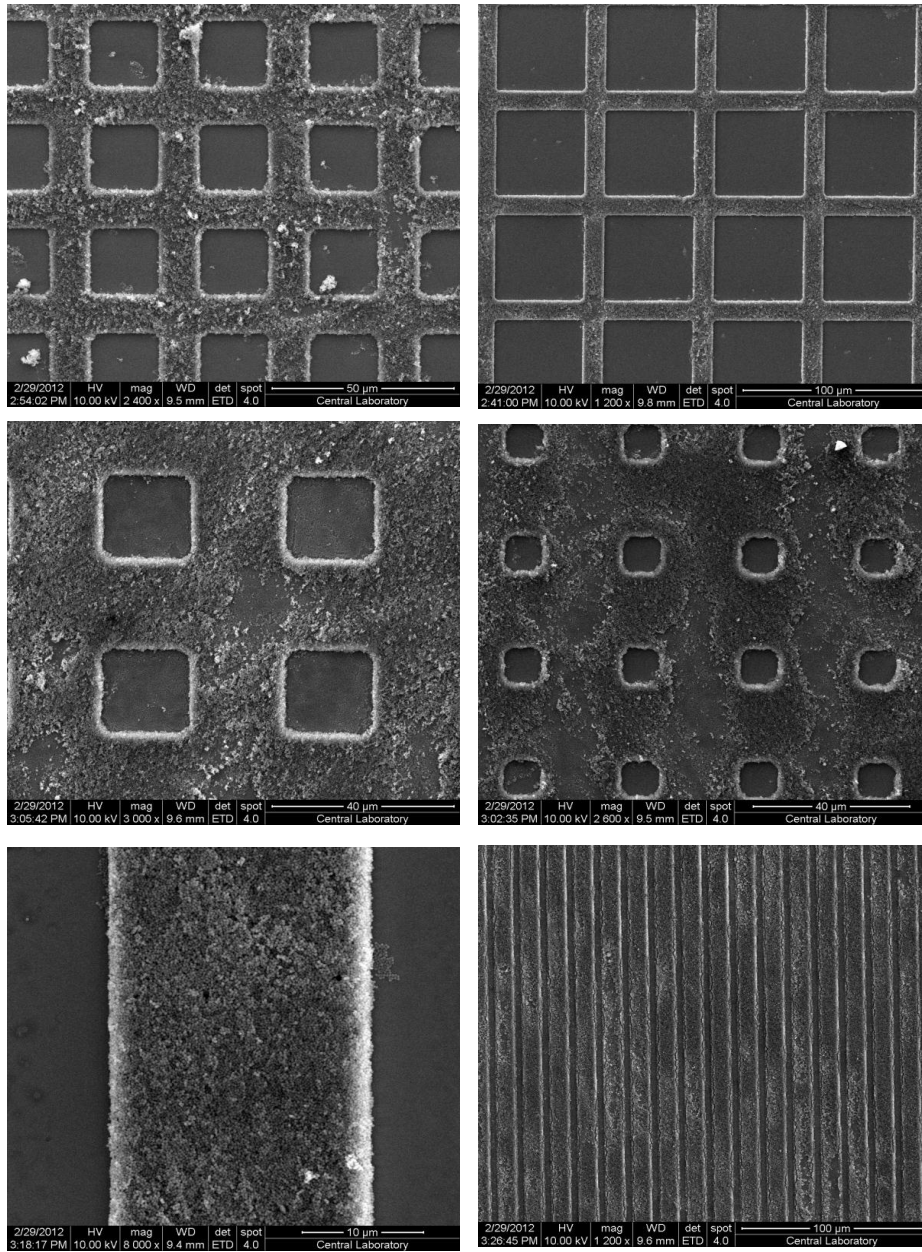


Figure B.2 Representative scanning electron microscopy images of prepared various zeolite patterns